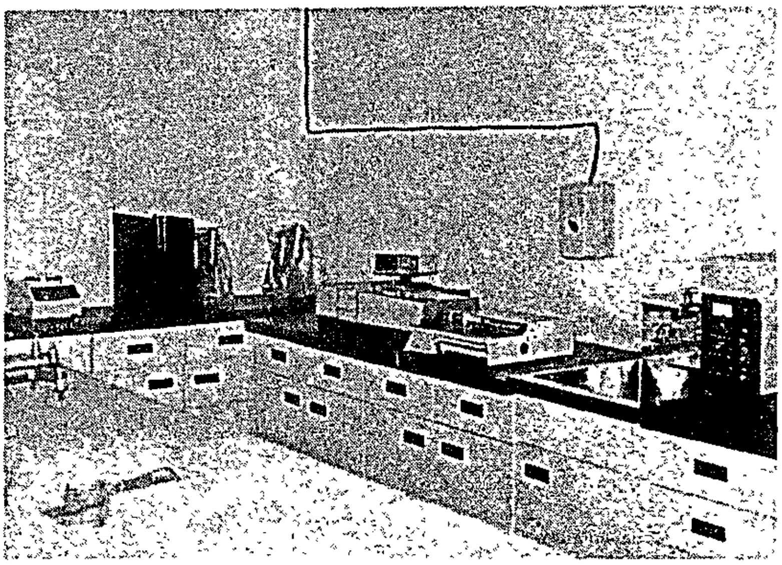

Foto-11 Fotoespectrómetro marca HITACHI en la sala de análisis químico.

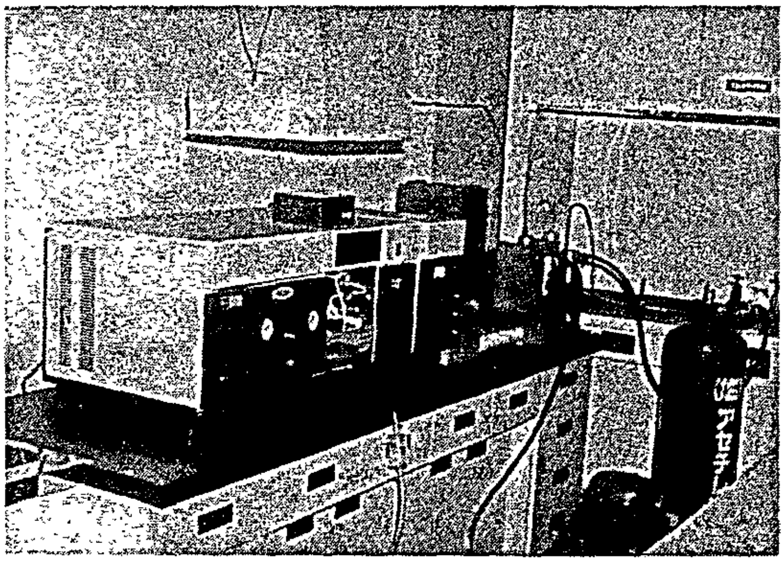

Foto-12 Absorcion Atómica/Fotoespectrometro de llama y parte de atras aparato de registro.

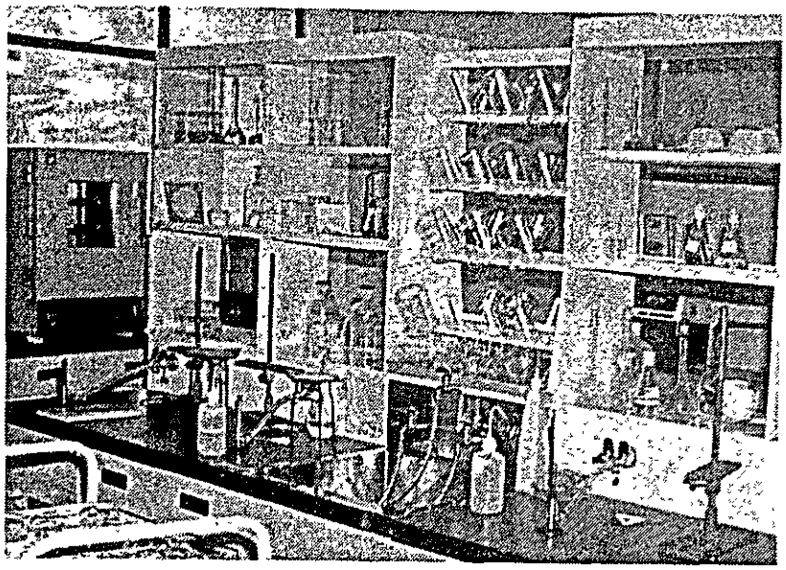

Foto-13 Mesa central de ensayo (parte central), atras secador de temperatura constante.

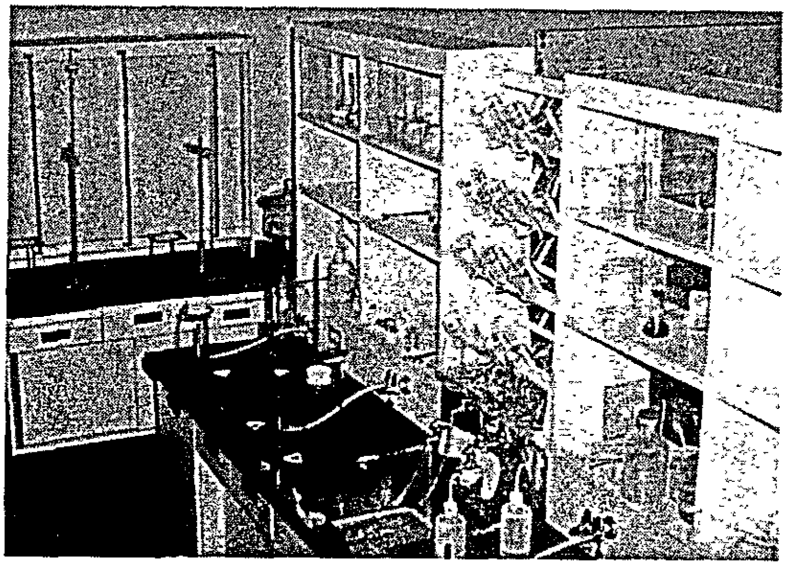

Foto-14 Mesa central de ensayo, atras aparato de titulacion.

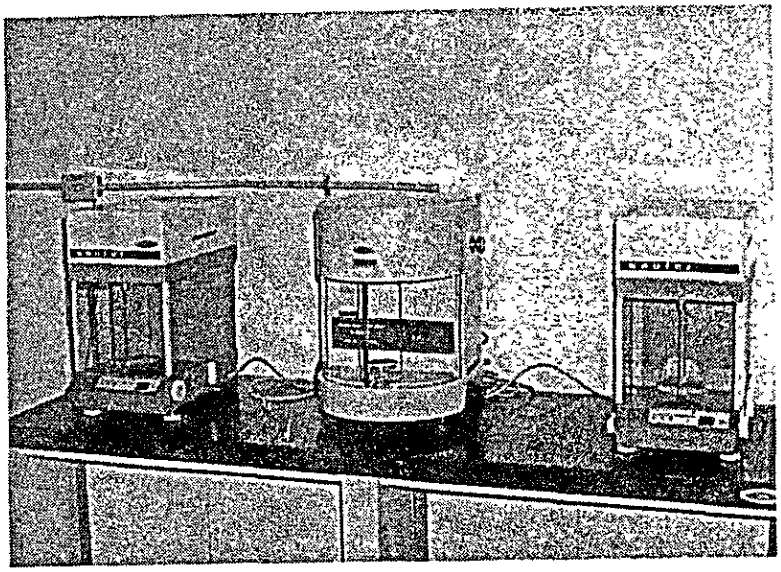

Foto-15 Dos balanzas de química Tipo SAUTER y una balanza marca SHIMAZU de sensibilidad ±0.1 mg.

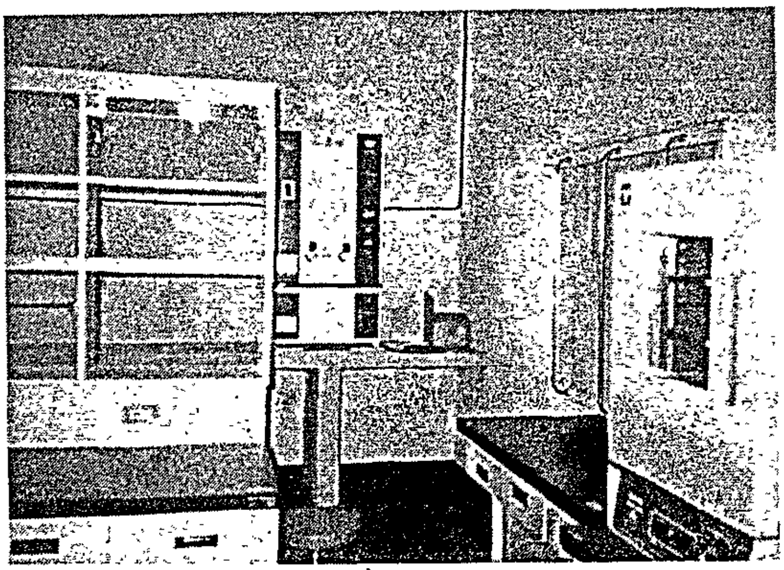

Foto-16 Secador de temperatura constante (borde derecha), aparato intercambiador de iones, destilador de agua.

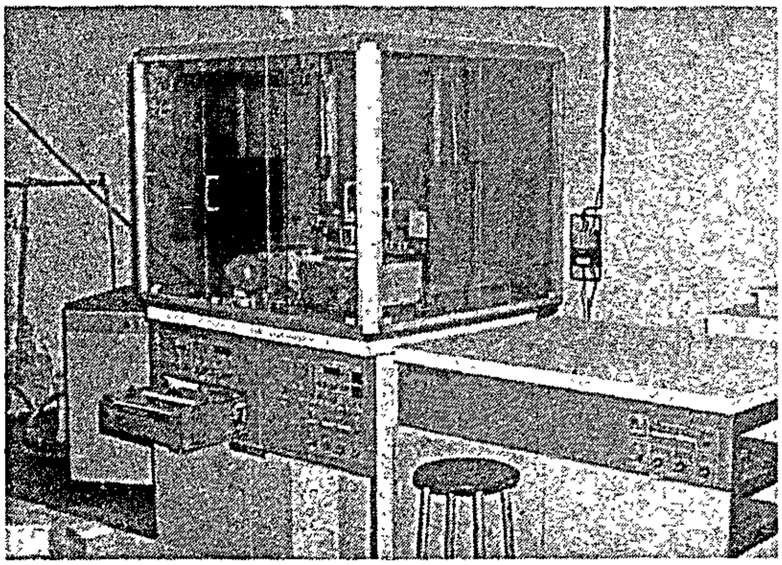

Foto-17 Equipo de difracción de rayos-X sobre polvo mineral RIGAKU DENKI.

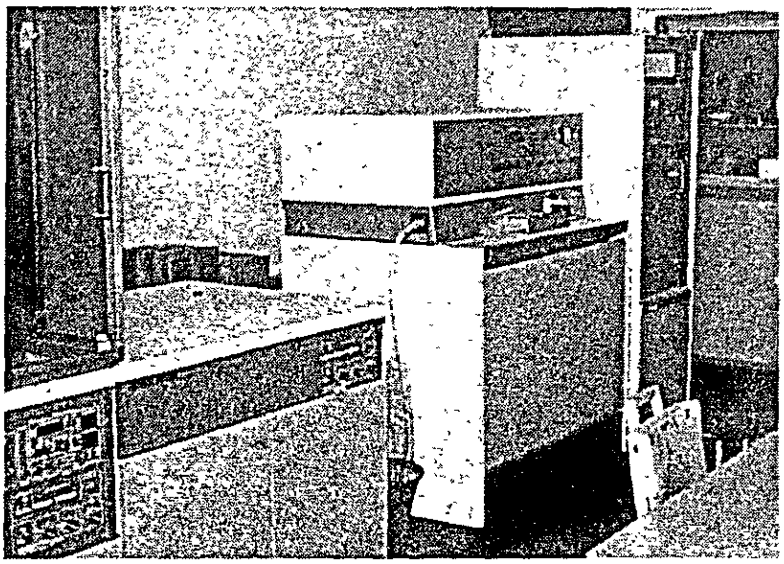

Foto-18 Equipo de análisis de fluorescencia de rayos-X RIGAKU DENKI.

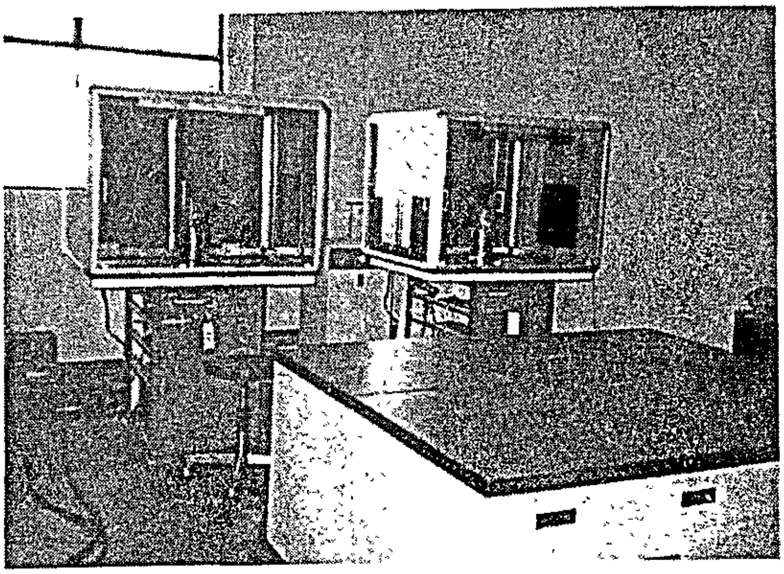

Foto-19 Dos generadores de rayos-X para Camara.

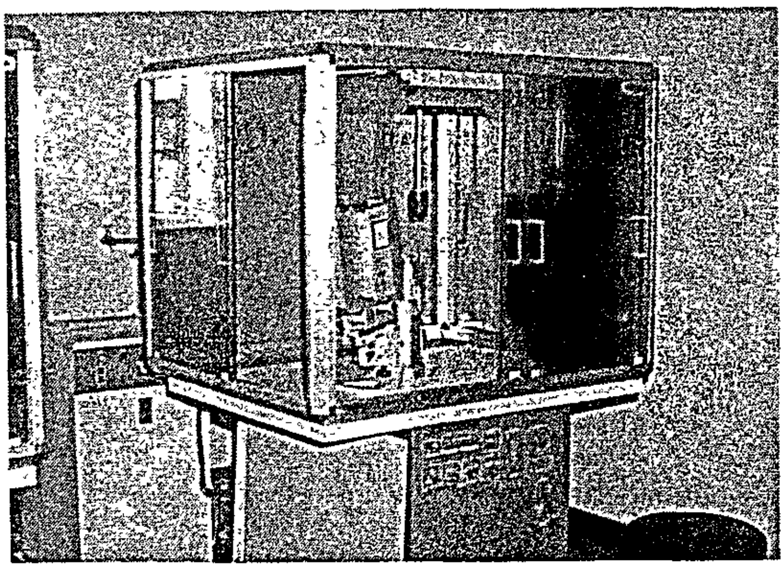

Foto-20 Camara de Guinier-Haag puesta sobre el generador de rayos-X.

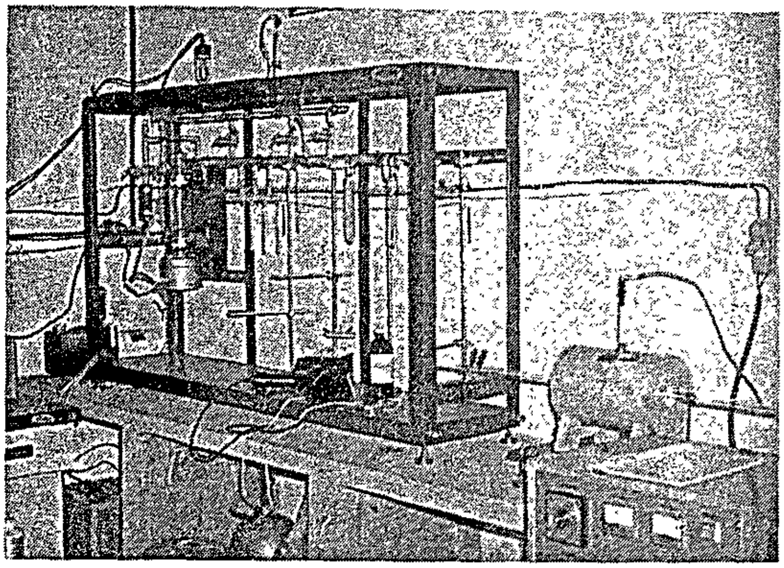

Foto-21 Aparato preparador de muestras de isótopos de azufre para análisis con espectrómetro de masa.

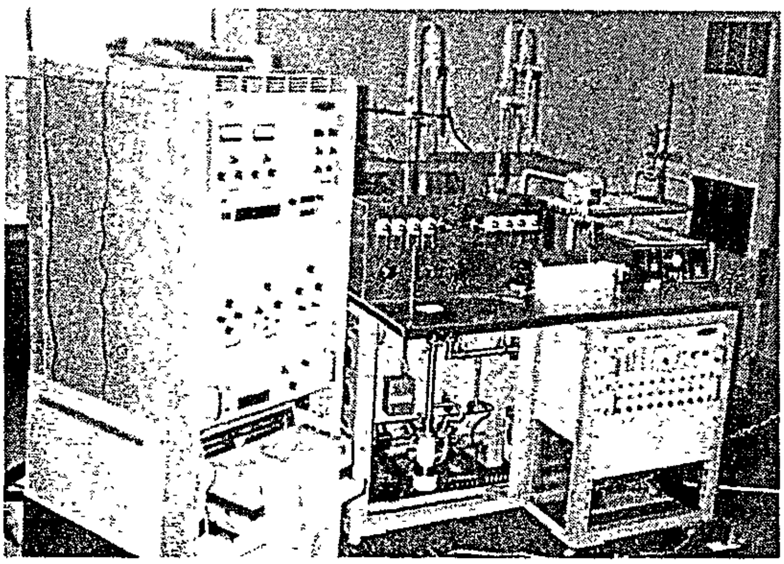

Foto-22 Espectrometro de masa, se usa principalmente para medir la proporción de isótopos de azufre.

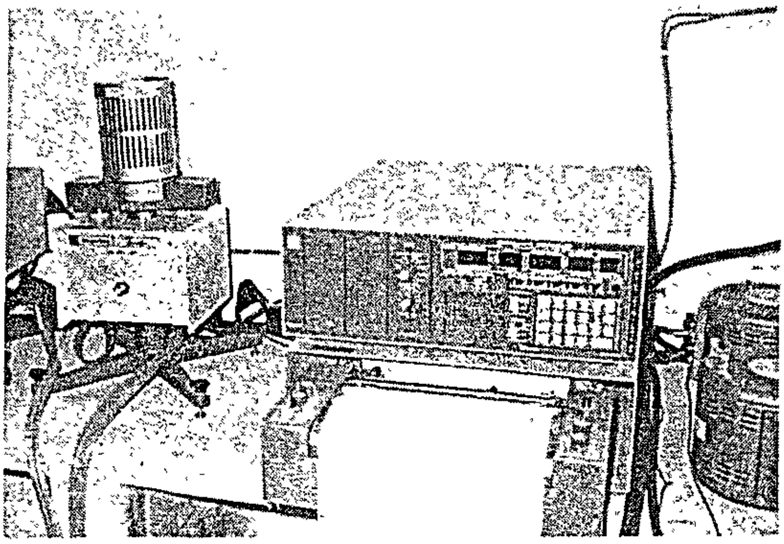

Foto-23 Equipo de análisis Térmico Diferencial RIGAKU DENKI.

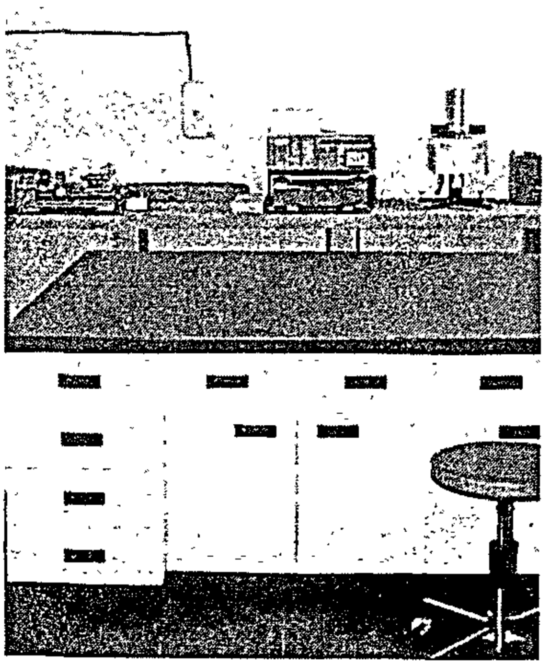

Foto-24 Equipo de análisis Térmico Diferencial y Mesotérmico RIGAKU DENKI:

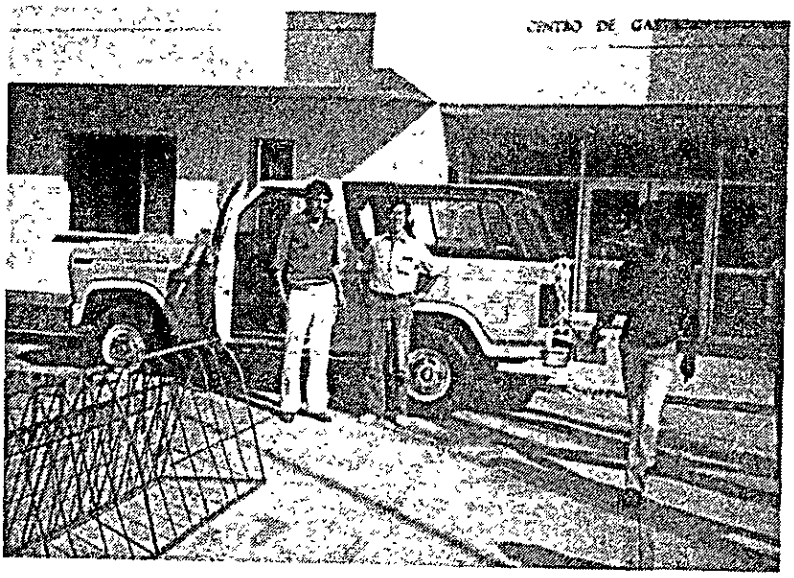

Foto-25 Foto de Jeep (Ford Bronco) y Sr. W. Vargas de JICA La Paz, Sr. I. Kobayashi frente al hospital de Gastro-entereología en Cochabamba.

Foto-26 Investigación de campo con el Jeep Toyota (cerro Ignimbrita parte oriental de la ciudad de Oruro), izquierda Ing. E. Soria, Sr. J. Castillo.

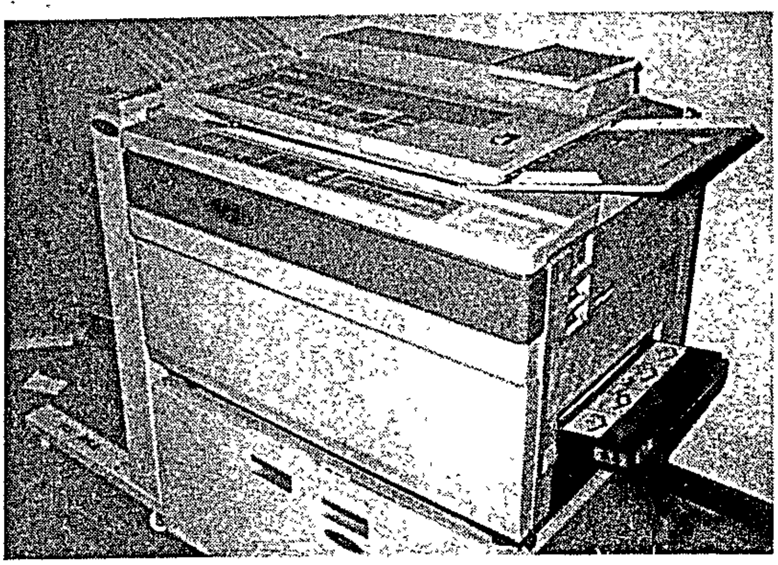

Foto-27 Copiador (Canon NP400).

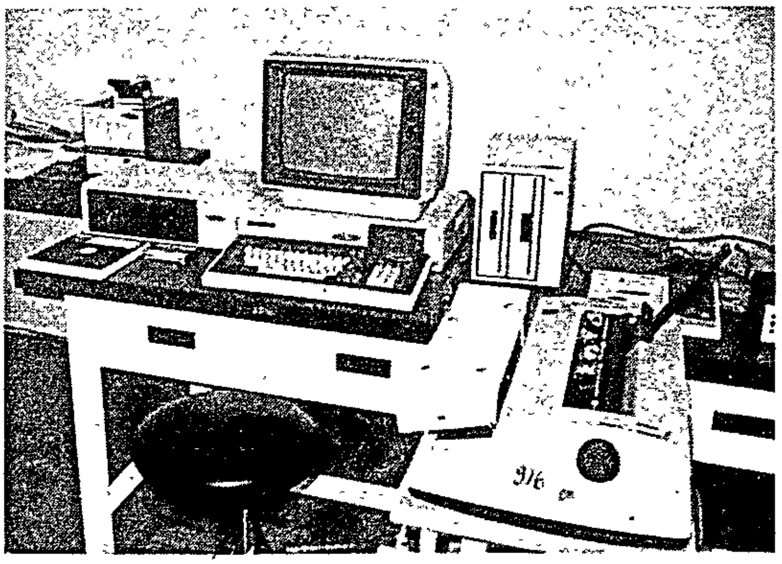

Foto-28 Micro computador NEC PC8800 sīstema, Flopy disco de 8", Mini flopy disco de 5", māquina de escribir IBM, Interface (KGS-80 y color display).

PARTE II

INFORME DE INVESTIGACION

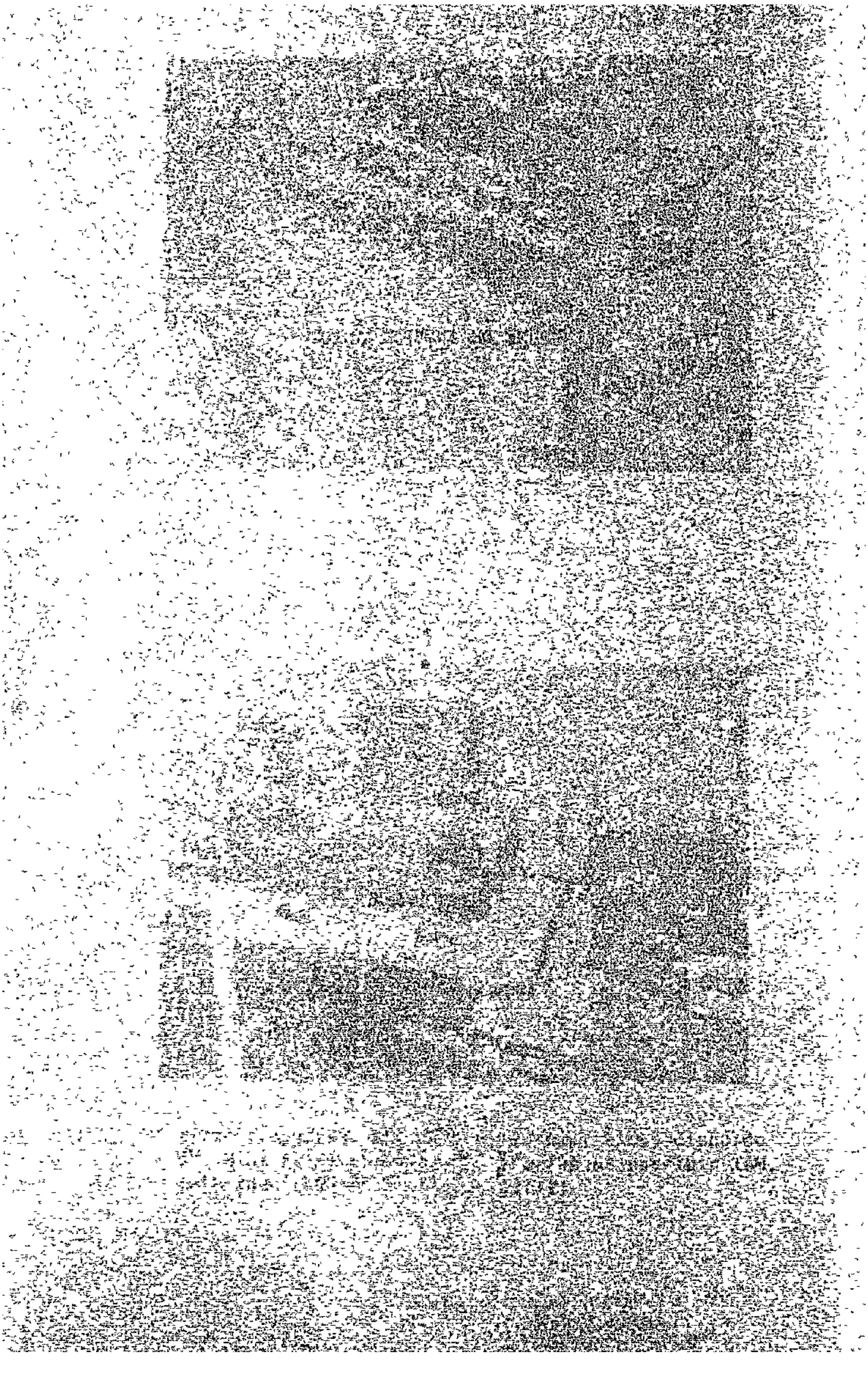

Ann.Rep.JICA-IGE/UMSA
Part II, 1, II-1-II-23, 1984

Chemical composition of granodiorite porphyry from San Pedro, and K-feldspar from Cerro Viscachani, Oruro, Bolivia

Tadato MIZOTA

Department of Mining and Mineral Engineering,
Yamaguchi University, Ube 755, Japan

Gary BECCAR, Freddy SAAVEDRA, Orlando SANJINES,
Alberto SANCHEZ AND Hernan VILLENA

Instituto de Geologica Economica, Universidad Mayor
de San Andrés, Cota Cota, La Paz, Bolivia

Eduardo SORIA

Instituto de Geodinamica y limnologia, Universidad
Mayor de San Andrés, Cota Cota, La Paz, Bolivia

Abstract

Granodiorite porphyry from San Pedro and K-feldspar from Cerro Viscachani, Oruro district, Bolivia, have been analysed by wet chemical method. The K-feldspar was found to be microcline from the X-ray diffraction data. The porphyry has been considered to be the main intrusive rock related to the mineralization of San Jose mine and the K-feldspar is the megacryst of the porphyry. The curing duration to make a precipitate of good filterability must be prolonged in comparison with that at sea level due to the low boiling temperature of water which is 85-86°C at Cota-cota district over 3300m in altitude. Burner temperature is insufficient for ignition of silica, R_2O_3 etc. due to the oxygen deficiency in the highlands, so electric furnance should be used frequently. The normative composition of the granodiorite porphyry and atomic ratio of the K-feldspar are given with the chemical compositions.

Introduction

In the training course of the wet chemical analysis in the Instituto de Geologia Economica, Universidad Mayor de San Andrés, two silicate samples have been analysed. One is K-feldspar crystal (megacryst) from Cerro Viscachani, San José mine district and the other is granodiorite porphyry containing K-feldspar megacryst from San Pedro quarry near San José mine. One of our object of this experiment has been to establish techniques for wet chemical analysis at highlands over 3300m, where the boiling temperature of water is almost 85°C.

Samples

Granodiorite porpyry

The granodiorite porphry occurs in stock-intrusive as the source of mineralization of San Jose and Itos mine (Sugaki et al. 1981). Most part of the rock is altered but we can find relatively fresh specimen at San Pedro quarry, northern part of Oruro city. The porphyry containes large amount of K-feldspare, frequently as megacryst, quartz, biotite and altered plagioclase as phenocrysts. The groundmass contains the same minerals as those of phenocrysts. The analysed specimen was selected from the part which is considered to be relatively fresh and dose not contain megacryst of K-feldspar.

K-feldspar

A large euhedral crystal with the longest dimension of about 3cm collected by F. Saavedra was crushed and pulverized directly, although it shows perthitic texture and contains small amount of biotite inclusions. The X-ray power data and calculated unit cell dimensions show that the feldspar is microcline (Table-1).

Table-1 X-ray diffraction data for K-feldspar from Cerro Viscachani, San Jose Mine, Oruro and the unit cell dimensions

d(obs)	d(calc)	I	h	k	l
6.60 A	6.63 A	15	1	1	0
6.53	6.54	11	0	2	0
4.23	4.22	13	2	0	-1
3.96	3.94	7	1	1	1
3.80	3.79	32	1	3	0
3.64	3.65	4	1	3	-1
3.48	3.49	21	1	1	-2
3.36		4	biotite		003
3.32	3.31	36	2	2	0
3.27	3.29	53	2	0	-2
3.245	3.240	100	0	0	2
3.205		13			
3.005	2.995	25	1	3	1
2.921	2.913	13 b	0	4	1
2.782	2.783	7	3	-1	-1
2.603	2.607	4	3	1	-2
2.587		11			
2.555	2.550	4	1	1	2
2.514	2.513	2	3	1	0
2.491	2.491	2	2	4	0
2.430	2.437	3	1	5	-1
2.384	2.382	2	3	-3	-1
2.330	2.329	2	1	-1	-3
2.178	2.180	45	0	6	0
2.129	2.125	4	1	5	-2
2.064		3			
1.972	1.967	3	3	3	-3
1.920	1.920	1	4	0	0
1.854	1.854	5	1	1	3
1.806	1.805	4	2	0	-4
1.800		13			
1.569	1.570	5	0	2	4

X-ray power data was taken by Ing.O. Sanjines, Cukα 1°/4min.-2θ

Cell Dimensions
a = 8.561 A
b = 13.08
c = 7.221
α = 90.37°
β =116.20
= 89.81

Unit cell dimensions were calculated by using LSUC/IGE program.

Method of analysis

The characteristic thing is that the analysis was carried out at highlands over 3300m where the boiling temperature of water is observed to be almost 85-86°C, although it varies slightly depending on the daily atmospheric pressure. This has a direct effect on the maturing of precipitate or growth rate of recrystallization and coagulation of gels which are fundamentally important for filtration or separation techniques. Prolonged time, almost 5 to 10 times longer than that at sea level, is necessary to obtain good filterability of a precipitate. Furthermore, we could not obtain a sufficiently high temperature to ignite silica, R_2O_3 etc. for gravimetric analysis using a gas burner due to the oxygen deficiency, so that we had to use an electric furnance for ignition treatment.

The details of the analysis were shown in the flowsheet as follows.

1. Outline of the analysis

1.1 Main flowsheet of the wet-chemical analysis

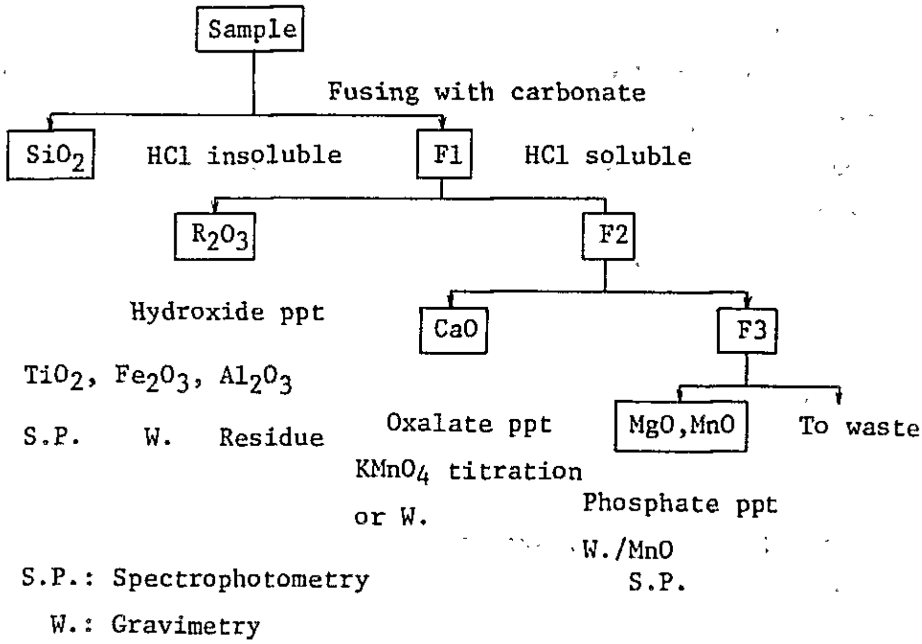

1.2 Partial analysis using another part of the sample

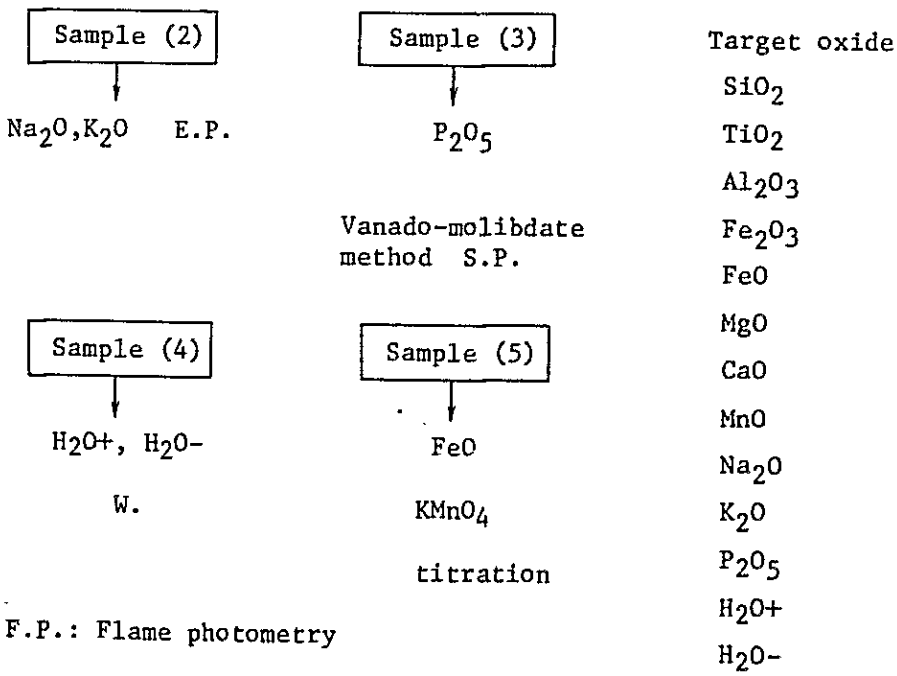

F.P.: Flame photometry

2. Flow sheet of the analysis

2.1 Main flow

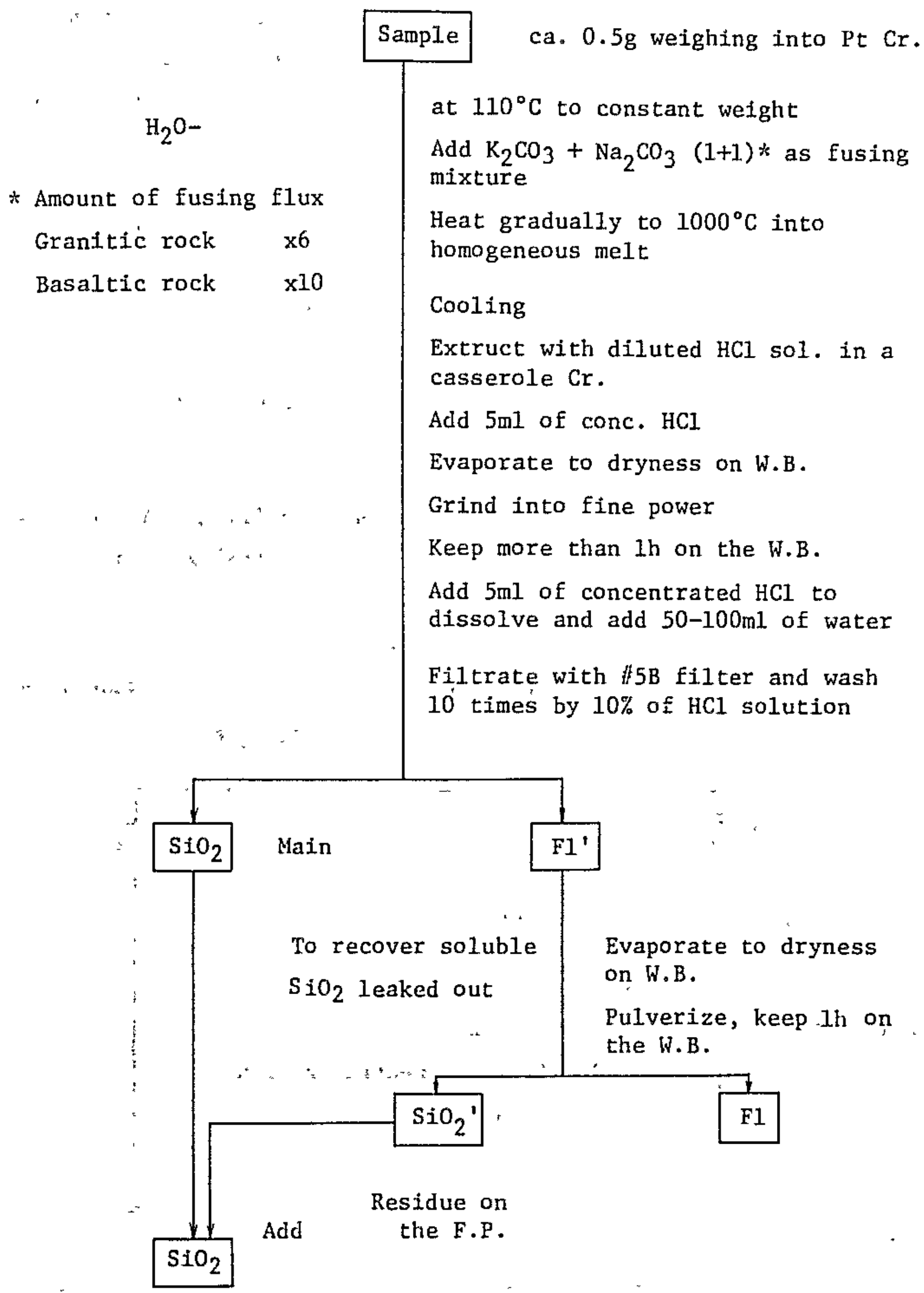

SiO_2

Put into Pt Cr. of const. wt. with the filter paper

Heat gradually. After F. P. is burnt out, heat up to 1100°C. Cool and weigh.

Repeat above to constant wt.

Add few drops of conc. H_2SO_4[1)] and 5ml of HF.

Evaporate on a sand bath

Repeat 2-times

Heat to ignition to constant wt.

To aboid evaporation of TiF_4 by the form of $Ti(SO_4)_2$

SiO_2 → Evaporation as SiF_4 SiO_2

X — Mainly R_2O_3 in the Pt Cr.

F1

Heat to nearly boiling. Add F.P. pulp.

Add NH_4OH(1+1) to newtralization

Add few drops exess

Boil for few minutes

Filtrate by #5B F. P. in hot, wash 10 -15 times with 2% of NH_4NO_3 sol.

The pressence of NH_4Cl is necessary to avoid the coprecipitation of $Mg(OH)_2$. High alkali condition dissolves $Al(OH)_3$.

→ R_2O_3: $Al(OH)_3$, $Fe(OH)_3$, $Ti(OH)_4$ etc.

→ F2'

Repurification (of R_2O_3):

Dissolve with dil. HCl

Heat to boiling

Add NH_4OH(1+1) to neutralization

Flitrate in hot.

→ R_2O_3

→ F2'' → F2

F2' → F2: CaO, MgO, MnO

F2

Heat to boiling
Add few drops of dil. HCl
Add 4% (almost saturated)
$(NH_4)_2C_2)_4$ 10-30ml

Newtralize with dil.NH_4OH
Boiling few min.
Stand for 4 - 24h for precipitation of
$CaC_2O_4 \cdot H_2O$
Filtrate with #5B F.P., Wash 3 - 4 times
with 0.1% $(NH_4)_2C_2O_4$ sol. and 3 - 4 times
with water

→ **Ca ppt** | → **F3'**

Ca ppt

$CaC_2O_4 \cdot nH_2O$
Dissolve into dil HCl sol., Boil
Add $(NH_4)_2C_2O_4$ sol. 2ml
Newtralize with NH_4OH(1 + 4)
Boil for few min.
Stand for 4 - 12h 1)

Filtrate by #5B F. P.
and wash

→ **$CaC_2O_4 \cdot H_2O$** | → **F3''**

F3' + **F3''** → **F3**

$CaC_2O_4 \cdot H_2O$ purified

1) Recrystallization to purify the ppt.
to avoid coprecipitation of Mg and Mn.

F3: MgO, MnO

R_2O_3 — Pt Cr. containing X

R_2O_3

Heat with the F. P. in the Pt Cr. gradually to 900 - 1000°C to const. wt.

gives total R_2O_3.

Add $K_2S_2O_7$ powder (5 - 10 times of the wt of R_2O_3), dry[1], seal cap and heat at low temp. up to black fume[2] with the reaction at 750°C

The temperature shows faint reddish color at the bottom of the crucible, then R_2O_3 dissolve into homogeneous red melt.

Cool

Add few drops of conc. H_2SO_4[3], dissolve into hot water, Filtrate with #5B F.P., if necessary.

1) Dry carefully to avoid splashing due to the presence of water.
2) SO_3 fume
3) To avoid hydrolysis of Ti

SiO_2" — Passed through to be weighed after ignition

F5 — Al_2O_3, total Fe_2O_3, TiO_2, (MnO)

F5 — Al_2O_3, TiO_2, total Fe_2O_3

250ml of M. F.

Pipette out and divide into 3-portions

50ml	50ml	150ml
for Ti	for Mn	for total Fe

F3 — in 500ml beaker

Neutralize with (1+4)NH_4OH

Add 15ml of $(NH_4)_2HPO_4$ saturated (-10%)

Add conc. NH_4OH upto 1/10 amount of the whole sol. Stir with "policeman"

Settle for 6 - 24h

Filtrate with #5C F.P.

→ **Mr, Mn ppt.** / → **To waste**

Mr, Mn ppt.

$MgNH_4PO_4 \cdot 6H_2O$, $Mg_3(PO_4)_2$, $Mg(NH_4)_4(PO_4)_2$ etc.

Dissolve into dil. HCl(1+4)

Add few ml of $(NH_4)_2HPO_4$ sol.

Neutralize with NH_4OH(1+4)

Add conc. NH_4OH by 1/10 amount

Stir

→ **Mg, Mn ppt. purified** / → **To waste**

Mg, Mn ppt. purified

(Mg, Mn) $NH_4PO_4 \cdot 6H_2O$

2.2 Quantitative determination of each element

2.2.1 CaO

1) $KMnO_4$ titration method

$CaC_2O_4 \cdot H_2O$ purified	on filter paper

- Wash down into a 300ml beaker by hot water
- Add H_2SO_4 into 1 - 1.5N
- Heat to 80°C
- Titrate with 0.1N $KMnO_4$ sol. above 60°C

2) Gravimetric method

$CaC_2O_4 \cdot H_2O$ purified	with filter paper

- Burn in a Pt Cr. of const. wt.
- Heat to ignition
- Weigh as CaO

When considerable amount of Mn exists in the Ca ppt., the ppt. is dissolved in diluted H_2SO_4 solution and the Mn is determined by the spectrophotometric method mentioned below.

Mg, Mn ppt purified

Don't use Pt. C

$MgP_2O_7 + MnP_2O_7$

- Burn in a Porceline Crucible of constant weight
- Heat to ignition to const. wt.
- Dissolve into dil. HNO_3 (1.2ml/ml)
- Add H_3PO_4 0.1ml[1)]
- Add $HgSO_4$ sat. sol. few drops.[2)]
- Add $AgNO_3$ 1ml[3)]
- Boil
- Add $(NH_4)_2S_2O_8$ 1g

The solution becomes purplish red of MnO_4^+ ion

↓ Pore into 50 or 100ml M. F.

S. P. at 525 - 530 mμ

2.2.3 Total Fe_2O_3

$SnCl_2$ reduction method

F_4 150ml

- Heat to boiling
- Make neutral with NH_4OH (1+4), $Fe(OH)_3$ ppt.
- some drops excess
- Boil to complete the ppt.
- Filtrate with F.P. #5B

→ filtrate: to waste

F_5

- Wash back the ppt to former beaker
- Add 10 ml of HCl (1+1), heat and evaporate until 5-10ml of the solution
- Reduce with $SnCl_2$ solution[1)] in hot by dropping one by one, add 1-2 drops excess. $Fe^{3+} \rightarrow Fe^{2+}$
- Cool quickly with cold water.
- Add $HgCl_2$ saturated solution (5ml) and shake.
- Dilute with 200-300ml of cold water.
- Add 25ml of MnO_4 Solution[2)].
- Titrate with 0.1 or 0.5N $KMnO_4$ standard solution with shaking the sample solution.

1) $SnCl_2$ solution

Conc. HCl, 100ml, in a beaker, add crystalline $SnCl_2$, 50g, and dilute with distilled water to 1ℓ after dissolution.

2) $MnSO_4$ solution

Crystalline $MnSO_4$ 67g + 600ml of water +H_3PO_4(S.G.=1.70) 138ml + H_2SO_4 130ml → 1ℓ with d.w.

$HgCl_2$ saturated solution is used for oxidizing the excess Sn^{2+} by Hg^{2+}.

2.2.4 TiO_2 (Hydrogen peroxide method)

F4 50ml

H_2SO_4 will be added finally at 10%.

H_2O_2(3%) sol. 5ml/50ml. --- yellow color

If it becomes hot, cool.

→ 100 ml meas.flask.

S.P. at 410-430mμ

If considerable amount of Fe^{3+} ion exists. few drops of H_3PO_4 is added to avoid the interference of yellow color by Fe^{3+} ion.

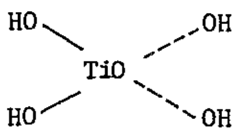

complex ion is considered in the solution by showing yellow.

The temperature should be constant at a colorimetric measurement, because the absorbancy is influenced by the temperature of testing solution.

Standard sol.: Extra pure grade of TiO_2 is ignited in Pt. Cr. to constant wt., fused with $K_2S_2O_7$ and dissolve into H_2SO_4 sol. 12-13ml/250ml. This solution is used for standard by pippetting out, diluting and coloring by the method mentioned above.

3. Partial analysis by other part of the sample

3.1 FeO

Weigh sample power Ca. 0.5g in Pt. Cr.

Prepare the following sol.: 100ml of deoxygenated d. w. in 200ml beaker, dissolve a spoonful of Boric acid (H_3BO_3), H_2SO_4 acidic about 1N.

The sample in Pt. Cr. is made wetty with d. w. deoxygenated by boiling. Add 2-3 drops of C.H_2SO_4 and HF 5ml. Put cover on the Pt.Cr. Heat weakly for 2-3 min. to decompose silicates. Be careful not to boil nor sprush.
Put it into the former beaker prepared and titrate with 0.1N $KMnO_4$ stand. sol.

Be careful by using the draft-chamber, because HF, hydrofluoric acid, is harmful for the creature.

Attention: Confirm that the decomposition is complete.

3.2 P_2O_5 (Vanado-molybdate method)

Weigh sample power of 0.1-0.2g in Pt. dish

Decomposition....Add conc.HNO_3 5ml, HF 5ml. Evaporate on a W.B. to dryness. Wash aroung inner wall of the dish and evaporate again. Add $HClO_4$ (percloric acid) 8mol[1)] 1ml. Evaporate fluoride and acid on a electric heating plate until the beginning of fume. Dissolve into 20-30ml of d.w. by boiling. If some insoluble materials are seen in it, it should be filtrate out in hot with 5B F.P. and wash few times with d.w. added 1 drop of $HClO_4$ for each time.

Coloration....Add 8mol $HClO_4$ 2.5ml, 0.02mol NH_4VO_3[2)] (ammonium metavanadate) 5ml, 0.2mol $(NH_4)_6Mo_7O_{24}$[3)] (ammonium molybdate) 10ml in the order → 50ml m.f. (yellow)

Wait for 30min before measuring by the S.P. method at 420mμ.

P_2O_5 Standard solution

Dissolve 0.4395g KH_2PO_4 (potasium dihydrogen phosphate) into d.w. up to 1ℓ. Reserve in a polyethylene bottle.

1) 8mol $HClO_4$ sol.....H_2O: conc$HClO_4$ = 14 : 86
2) 0.02mol NH_4VO_3 sol.....2.5g of NH_4VO_3 into boiling d.w. (500ml), cool, add conc.HNO_3 20ml → 1ℓ. Reserve in a polyethylene bottle.
3) 0.2mol $(NH_4)_6Mo_7O_{24}$ sol.....Dissolve 50g of $(NH_4)6Mo_7O_{24}\cdot 4H_2O$ or 65g of $Na_2MoO_4\cdot 2H_2O$ into d.w. at 50 C → 1ℓ.

Reserve in a polyethylene bottle.

The phosphorous content must be under 2.0mg/25ml, and the testing solution should be weakly acidic

3.3 Na_2O, K_2O (Flame photometry)

Sample power 0.1-0.2g in Pt. dish

Add HNO_3 3ml and HF 5ml. Heat on a hot plate up to fume. Cool and wash down around inside of Pt. dish. Evaporate HF and H_2O. Make acidic with HCl into 0.1mol sol. If there is insoluble material, it should be filtrate. Make under 70ppm of Na^+ content.

The wave lengths of flame photometric measurement: K 768mμ, Na 589 mμ.

K, Na standard solutions ..... NaCl and KCl are weighed separately in porcelain crucible of constant weight. Heat at 500°C for 1 hour, cool and weigh. This is repeate until we obtain the constant weight. Dissolve into d.w. in HCl acidic to avoid putrefaction. Reserve in a polyethylene bottle.

3.4 H_2O-, H_2O+

Sample 0.5g in Pt.Cr. of const. wt.

(H_2O-)

Weigh and heat at 110°C for 1 hour.

Cool for 30 min and weigh.

repeat above until we obtain the constant wt. which means the difference of weight from the preceding weight become smaller than ±0.1mg.

(H_2O+)

Heat to ignition and determine the weight loss of water. We must consider about the change, $Fe^{2+} \rightarrow Fe^{3+}$, occured by the ignition.

When the heated sample powder could not be detached from the Pt. crusible, add 5ml of HF, heat weakly until almost dryness in a draft chamber and wash out with water.

Results

P_2O_5 is not determined in this analysis. Two of the analyses for the one and the same sample of the K-feldspar and four for the granodiorite porphyry sample were carried out. The results in Table 2 shows the average value for these analyses, where apparently abnormal values are excluded from the averaging calculation.

K-feldspar

This feldspar is considered to be microcline from the results of X-ray diffraction (Table 1) and contains much amount of trace elements such as Fe^{3+}, Mg, Fe^{2+}. Especially, the amount of Al is too high in comparison with common K-feldspar. This comes from the presence of biotite inclusion and, probably, clay minerals as partial alteration products. The Or, Ab and An can be calculated to be 71.4, 24.5 and 4.1%, respectively.

Granodiorite porphyry

The silica content of this rock is slightly lower than usual quartz porphyry which is widely distributed and has been called "quartz porphyry" in this area. Normative corundum and pyroxenes show the presence of biotite and clay minerals. The occurrence of acidic rocks in this area should be investigated in terms of chemical nature.

Table 2. Chemical composition of K-feldspar from Cerro Viscachani and granodiorite porphyry from San Pedro quarry, San Jose mine, Oruro

Granodiorite porphyry

Oxide	wt. %	Norm. mineral	wt. %
SiO_2	66.31	Qz	23.53
TiO_2	0.13	Il	0.25
Al_2O_3	18.01	C	4.48
Fe_2O_3	0.81	Mt	1.19
FeO	2.52	Fs	3.88
CaO	1.95	En	2.96
MnO	0.04	An	9.84
MgO	1.17	Or	20.91
K_2O	3.48	Ab	32.95
Na_2O	3.83	Total	99.99
H_2O+	0.85		
H_2O-	0.18		
Total	99.27		

K-feldspar

Oxide	wt. %	Metal	(as O=32)	
SiO_2	62.25	Si	11.453	16.239
TiO_2	0.04	Al	4.712	
Al_2O_3	21.75	Fe^{3+}	0.068	
Fe_2O_3	0.49	Ti	0.006	
CaO	0.71	Mg	0.063	3.573
MnO	0.01	Mn	0.002	
MgO	0.23	Na	0.848	
K_2O	10.54	Ca	0.140	
Na_2O	2.38	K	2.471	
H_2O+	0.33	Fe^{2+}	0.049	
H_2O-	0.04			
Total	99.09			

Acknowledgement: One of the authors (T.M.) is greately indebted to Dr. H. Konno of Tohoku University for his teaching on the method of chemical analysis.

Reference

Sugaki, A., Ueno, H., Shimada, N., Kitakaze, A., Hayashi, K., Shima, H., Sanjines, O. V. and Saavedra, A. M. (1981), Geological study on polymetallic hydrothermal deposits in the Oruro district, Bolivia. Sci. Rep. Tohoku Univ., Ser. III, XV, 1-52.

Bolivia国オルロー市，San Pedro花崗閃緑斑岩及びCerro Viscachani産カリウム長石の化学組成

溝田忠人，G.ベッカー，F.サーベドラ，O.サンヒネス，
A.サンチェス，H.ビレナ，E.ソリア

ボリビア国オルロ地区のSan Pedro 花崗閃緑斑岩及びCerro Viscachani産カリウム長石が，湿式法により分析された。カリウム長石は，X線データによりマイクロクリンであることがわかった。花崗閃緑斑岩は，San Jose鉱山の鉱化作用に関係する主要な貫入岩と考えられている。適切なろ過性をもつ沈殿を作るための熟生時間は，3,300mを越すCota－Cota 地区の標高で，水の沸点が85－86℃であるために，海水面レベルにおけるより長くしなければならなかった。酸素不足のため，バーナーの温度が上らず，シリカやR_2O_3の強熱は不可能で，しばしば，電気炉を用いなければならない。岩石のノルム組成，長石の原子比が，化学組成と共に示されている。

Composición Química del Feldespato Potacio del Cerro Viscachani, y del Pórfido Granodiorítico de San Pedro de la Ciudad Oruro´ Bolivia

Tadato Mizota, Gary Beccar, Freddy Saavedra, Orlando Sanjinés, Alberto Sánchez, Hernan Villena, E. Soria

El feldespato potacio del Cerro Viscachani y el pórfido granodioritico fueron analizado por via humeda. Este feldespato fue determinando como microclina por los datos de difracción de rayos-X. Este porfido granodioritico es uno de los mas importantes rocas intrusivas relacionados con los depositos minerales de la mina San José. El punto de ebullción de agua en Cota Cota es 85°-86°C porque esta área está a una altura promedio 3,500m s.n.m. Por lo tanto, para hacer buen precipitado en esta altura necesita un tiempo más largo que en una lugar del nivel del mar. A falta de oxigeno no es posible calentar silica o R_2O_3 hasta alta temperatura adequada por soplete; a veces es necesario usar horno eléctrico. Se han dado la composición NORMA del roca, la razon atomica del feldespato y las composiciones químicas de ambos muestras.

Ann.Rep.JICA-IGE/UMSA
Part II, 1, *II-24-II-44, 1984*

Petrological Study of Sajama Volcano in Bolivia

Setsuya NAKADA

Department of Geology, Faculty of Science, Kyushu University, Fukuoka, 812, Japan

Eduardo SORIA E.

Instituto de Geodinamica y Limnologia, Universidad Mayor de San Andrés, La Paz, Bolivia

Abstract

Sajama Volcano (6,542m above the sea level), Oruro, Boliva, is a compound volcano with several parastic cones. The parastic cones and the summit of the volcano are arranged in the direction of N70°E-S70°W. The activity of the parastic cones moved toward the summit of the volcano. The rocks from the parastic cones are augite-biotite dacites, and, characteristically, include sphene phenocrysts. The older rocks among them are more basic and contain large amounts of hornblende phenocrysts, while the younger ones cantain sanidine phenocrysts. Plagioclase phenocrysts are classified into normal and dusty types. It is considered that the latter resulted from the mixing of magmas with different compositions.

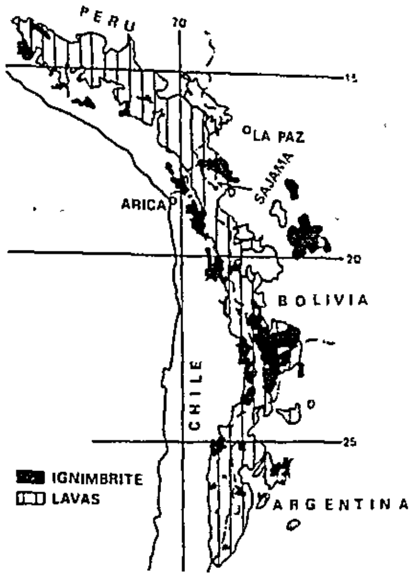

Fig. 1 Distribution of Upper Cenozoic volcanic rocks in the central Andes (after Baker, 1981)

Introduction

Nevado Sajama is a large volcano in the Oruro province in Bolivia, near the frontier with Chile (Figure-1). The volcano is compound stratovolcano with various parastic cones (IUGG, 1971). It is situated in the middle part of the central Andes volcanic belt which runs from 13°S to 19°S along the coastal line between Southamerican continent and Pacific Ocean. The Peru-Chile trench axis lies 95±25 km off shore. The subduction of Nazca plate below the Southamerican continental plate occurs in the direction of N80°E at a convergent rate of about 11 cm/yr (Nur and Ben-Avraham, 1981). The estimated thickness of the crust under the central Andes volcanic belt reaches up to 70 km (James, 1972). The central Andes volcanic belt is characterized by the presence of andesite-dacite lavas and ignimbrites. These volcanic rocks have high contents of Si, K, Rb, Sr and Ba and higher Sr isotopic ratio, being compared with those in the north and south Andes volcanic belts (Thorpe and Francis, 1979). The K_2O content of volcanic rocks in the central Andes increases with the distance from the coastal line (Lefévre, 1973; Thorpe and Francis, 1979). Magmas which formed the central Andes are recently considered to have evolved in terms of assimilation and fractional crystallization by some investigators (e.g. Depaulo, 1981; Harmon et al., 1982; James, 1982).

This paper presents a preliminary petrographical aspect of Sajama Volcano about which no petrological study has been done.

Field characteristics

According to the list of the world active volcanos (IUGG, 1971), the name of this volcano is NEVADO DEL SAJAMA with the world volcanic map's reference number of IV-88. There is no eruption record. The summit of the volcano is located at 18°07'S and 68°53'W. Sajama Volcano covers an area of 240 km^2. Base level of the volcano is about 4,300 m above the sea level, while the height of the summit of the volcano is 6,542 m. The volcano is conical with several parastic cones in the direction of N70°E-S70°W (Plate 3 and Figure-2). The top of the volcano is covered with glaciers and snow (Plates 1 and 2), which makes an exhaustive sampling of lavas near the summit difficult or impossible. The upper parts of the flank of the volcano (5,000 to 6,000 m) were deeply eroded by glaciers and are very steep. Several U-shaped valleys which taper downward run radially from the summit. Some knife-edged divides with pyramid-shaped peaks survive near the top of the volcano. Interior structure of the volcano is able to seen in the wall of deeply eroded valleys (Plate 2). Some parts of the wall are colored in yellow, indicating the evidence of solfatara.

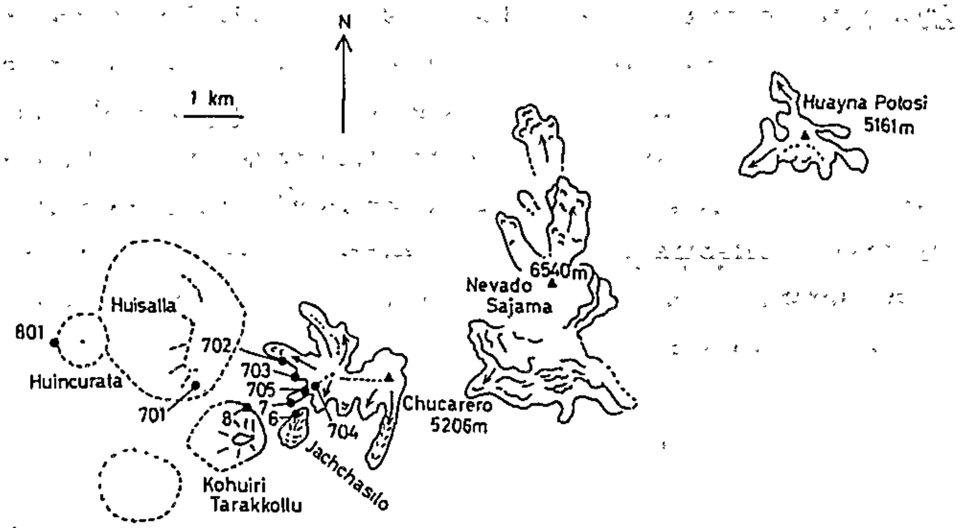

Fig. 2 Distribution of parastic cones and summit lavas of Sajama Volcano and the sampling localities.

Some structures of the summit lavas and the parastic cone lavas are able to be read by aerial photographs. Since the summit is completely covered with glaciers and snow, topographic feature of summit crater is not observed. However, topograph of snow-covered surface shows that several lava flows run down northward. The front of the lava flows is not covered with snow, and rides on the ridge eroded by glaciers. The surface structure of the front of the lava flow shows the age of the activity resemble to the those of the younger parastic cones (Chucarero and Huayna Potosi). Some units of lava flows of the summit lavas are able to be recognized also in the east or south of the summit (Figure-2). By only aerial photographs, however, it is difficult to read whether the age of the activity of the lava flows is younger or older than the glacier erosion age. Chucaroro and Huayna Potosi are young parastic cones. Flow structures of the lavas of the both cones are very clear in aerial photographs, as shown in Figures-2 and 3. The lavas are blocky. Chucarero lavas were emitted from two points, while Huayna Potosi lavas from one point. Huayna Potosi lavas ride on the ridge eroded by glaciers.

Jachchasilo parastic cone is lava dome with small lava flows in the southern flank (Figure-3). The dome is a little older than or as young as Chucarero lavas. Kohuri Tarakkollu is older than the lavas described above. Flow structure of Kohuri Tarakkollu lavas is not clear. This one has a couple of summit crater Figure-3). Huisalla and Huincurata parastic cones are older than Kohuri Tarakkollu and deeply dissected. Furthermore old parastic cone is located south of the Huisalla cone.

Fig. 3 Detail structures of parastic cones of Chucarero, Jachchasilo and Kohuiri Tarakkollu, which were read from aerial photographs. Small solid circles show the emittion points of lavas of Chucarero parasic cone.

According to the principle by Nakamura (1977), the distribution of parastic cones around the main volcanic center (summit-crater of caldera) reflects the maximum horizontal tectonic stress. When volcanic field is under the compressional tectonic stress field, owing to a collision of oceanic plate against the continental plate, the direction of the arrangement of the parastic cones is nearly parallel to the direction of the collision. The parasitic cones and the summit of Sajama Volcano line up in the direction of N70°E. This direction is close (but not equal) to the estimated direction of the subduction of Nazca plate (N80'E).

Table 1 Phenocryst assemblage of lavas of parastic cones and mineral assemblage of cognate xenolith.

Name of lava	ol	hyp	aug	hor	biot	N-pl	D-pl	Q	san	sph	Remarks
Chucarero	-	+	++	-	+++	+++	++	++	+	-	Cristobalite in g.m.
Jachchasilo	-	+	++	+	+++	+++	+	++	+	++	
Kohuiri Tarakkollu	-	-	+++	+	+++	+++	-	-	+	++	
Huisalla	-	+	++	+++	+++	+++	++	+	-	+	Cristobalite in g.m.
Huincurata	-	-	+++	+++	+++	+++	+	-	-	+	Cristobalite in g.m.
Xenolith	+	+	++	+++	+	+++	-	-	-	+	Cristobalite

Abundances of individual phenocrysts decrease in the order from +++ to +. - means no appearance. ol:olivine, hyp:hypersthene, aug:augite, hor:hornblende, biot:biotite, N-pl:normal-type plagioclase, D-pl:dusty-type plagioclase, Q:quartz, san:sanidine, sph:sphene. g.m. means groundmass. Xenolith is in Huincurata lava.

Petrography

Rock samples were taken from five parastic cones shown in Figure-2. The petrographical characters of theses lavas are described below. Phenocryst assemblage is listed in Table 1. Grain sizes of phenocrysts are less than 2.5 mm. Relatively large large crystal, up to 0.5 mm long, of apatite is common in these lavas. Associated opaque mineral is magnetite.

Chucareoro lava

Phenocrysts of quartz, sanidine, plagioclase, augite, hypersthene and biotite are embedded in groundmass with intersertal texture (Plate 4). Quartz phenocrysts are corroded. Plagioclase phenocrysts are divided into two types; one is euhedral clear crystal (normal type) and the other is corroded crystal with dusty marginal zone (up to 0.2 mm wide) along the crystal surface and with clear interior part (dusty type). Dusty zone contains many, very fine channels and inclusions of glass. Dusty-type plagioclase has always very clear; narrow (up to 0.03 mm wide) overgrowth rim (Plates 4, 10 and 11). Some aggregates of plagioclase have dusty zone in their marginal part, but each grain has no dusty zone. Augite phenocrysts have pleochroism of yellow green, while hypersthene phenocrysts is pale green. Biotite phenocrysts have the axial color of deep brown red. Many mafic minerals are oxidized. In the groundmass, there are aggregates of cristobalite.

Jachchasilo lava

Phenocrysts of quartz, sanidine, plagioclase, augite, hornblende, biotite and sphene are embedded in glassy groundmass. The glass is partly devitrified and has the orb texture (spherulite texture; Plate 5). Quartz phenocrysts are resorbed. Dusty-type of plagioclase is rarely observed. Hornblende phenocrysts have the axial color of reddish brown and are usually small crystal with skeletal form. Sphene phenocrysts are large and euhedral, up to 1 cm long.

Kohuri Tarakkollu lava

This lava also contains large crystal of sphene (Plate 6). Groundmass is glassy and shows orb texture. Normal-type plagioclase is only observed. Augite phenocrysts have the pleochroism of pale green and 2Vz of about 40°. Hornblende phenocrysts have the Z-axial color of reddish brown. X and Y (or Z) axial colores of biotite phenocrysts are yellow brown and dark brown respectively. Sanidine phenocrysts are present in small quantities. Sphene includes apatite and zircon crystals.

Huisalla lava

The rock contains the phenocrysts of quartz, plagioclase, hypersthene, augite, hornblende, biotite and sphene in the intersertal groundmass (Plate 7). Quartz phenocrysts are corroded. Hornblende phenocrysts show hollow or skeletal form and are opacitized. The Z-axial color of hornblende phenocrysts is brown. Sphene is present in small amount. Cristobalite crystals are embedded in groundmass.

Huincurata lava

The rock contains phenocrysts of plagioclase, augite, hornblende, biotite and sphene (Plate 8). Groundmass is intersertal and includes aggregates (about 1 cm across) of cristobalite. Most of plagioclase phenocrysts are dusty type, while plagioclase microphenocrysts are all normal type. Augite phenocrysts are zoned strongly and sometimes corroded. The Z-axial color of hornblende phenocrysts which usually show hollow form is dark yellow green. Large crystals of hornblende include augite in their core. Biotite has the pleochroism of X=pale yellow brown and Y or Z=dark reddish brown.

Xenolith

In Huincurata lava, some cognate xenoliths with the diameter of about 1 cm are contained (Plate 9). The xenoliths are holocrystalline and dioritic in composition. Constituent minerals are always smaller (less than 1.5 mm long) than the phenocrysts of the host lava. The texture is subophitic. Plagioclase, olivine, hypersthene, augite, hornblende, biotite and sphene are included. Aggregates of cristobalite fill space among the above minerals. Plagioclase is subhedral and clear prismatic crystal. Olivine crystal is fringed with crystals of biotite and augite. Augite shows pale green. Hornblende is skeletal and brownish. Biotite has the pleochroism of X=yellow brown and Y (or Z)=reddish brown. Elongated and euhedral crystal of sphene is observed in small quantity.

All rocks are augite-biotite dacite. Sanidine phenocrysts occur in the younger parastic cone lavas. Most of rocks contain skeletal crystal of hornblende, but the older parastic cone lavas are enriched in hornblende. Some lavas are characterized by the presence of sphene phenocrysts or of groundmass cristobalite. Proportion of dusty-type plagioclase to normal-type plagioclase in amount has no relation with the age of volcanic acitivity (Table 1). It seems that the lava with large phenocrysts of sphene includes small amount of dusty-type plagioclase.

Normal-type plagioclase and interior part of dusty-type plagioclase have scarcely oscillatory zoing. Mean composition of the normal-type plagioclase is An_{50}, which was determined by the method of Suwa et al. (1974). On the other hand, core composition of dusty-type plagioclase is about An_{35}. Its rim composition is about An_{45}. That is, dusty-type plagioclase is reversely zoned in its marginal part.

Eichelberger (1978) suggested that corroded plagioclase with dusty zone and clear, calcic overgrowth rim is the evidence of magma mixing between rhyolitic and basaltic magmas. Sodic plagioclase which crystallized from rhyolitic magma was resorbed in mixed magma, but was surrounded by more calcic plagioclase precipitated rapidly from the mixed magma. The presence of dusty-type plagioclase, skeletal hornblende and strongly zoned, corroded augite together with the unique phenocryst assemblage consisting of so many kinds of mineral in Sajama volcanic rocks, may indicate that the magma originated from mixing of magmas with different compositions.

In volcanic rocks, sphene is less common, but small crystals were reported in phonolite (Phillips and Griffen, 1981). The occurrence of sphene phenocrysts in calc-alkaline dacite like Sajama volcanic rocks has not been reported. In the present volcanic rocks, sphene is euhedral and occurs as large phenocryst. The cognate xenolith also includes euhedral crystal of sphene. The sphene crystal may have been precipitated directly from Andean acid magma, or, alternatively, may have been a melting residue of plutonic rocks under Sajama Volcano.

Table 2 Major chemical composition of Sajama volcanic rocks.

	704	801	CIPW norm**	704	801
SiO_2	66.24	63.33	Q	18.2	12.6
TiO_2	0.79	0.91	or	26.1	22.5
Al_2O_3	14.84	15.25	ab	33.6	36.4
$Fe_2O_3^*$	4.20	5.00	an	10.2	11.6
MnO	0.06_1	0.07_3	di	2.3	5.2
MgO	1.47	2.35	en	3.1	4.5
CaO	2.90	3.92	fs	3.1	3.5
Na_2O	3.92	4.25	mt	1.2	1.3
K_2O	4.36	3.76	il	1.5	1.7
P_2O_5	0.25	0.27	ap	0.6	0.6
Total	99.03	99.11		99.9	99.9

*Total iron as Fe_2O_3. **Recalculated to 100% (without water), and assumed that 20% of total iron were Fe_2O_3. 704:Chucarero lava(SN83090704) 801:Huincurata lava(SN83090801)
Analytical method:Nakada,S.,Yanagi,T.,Maeda,S., Fang,D. and Yamaguchi,M.(1984)X-ray fluorescence analysis of major elements in silicate rocks. *Sci.Rep.Fac.Sci.Kyushu Univ.,(D),in press.*

Chemistry

Major element compositions of Chucarero and Huincurata lavas were determined by X-ray fluorescence spectrometer, Rigaku Geiger Flex: 3063P of Kyushu University. The sample powder was mixed with flux and then fuses. The detail of the analytical method will be shown in Nakada et al. (in press). The analytical results are listed in Table 2.

Both lavas are calc-alkaline, high-K dacitic and metaluminous (diopside normative) in composition. They show high alkali contents. Being compared with the average composition of island arc volcanic rocks, they are enriched in P_2O_5. The P_2O_5 enrichment reflects the high abundance of apatite in Sajama volcanic rocks. Though Huincurata lava contains sphene phenocryst, it is not especially enriched in both CaO and TiO_2. The rock from Chucarero parastic cone is more acidic than that from Huincurata. Kussmaul et al. (1977) discussed the relationships of K_2O and Na_2O contents of volcanic rocks in southwestern Bolivia, and showed that K_2O content increases eastward, while Na_2O decreases. Compositions of two lavas studied here are plotted above the average trends of the composition of southwestern Bolivia volcanic rocks in their K_2O- and Na_2O-longitude diagrams. That is, Sajama volcanic rocks are much enriched in both Na_2O and K_2O.

Summary

Parastic cones of Sajama Volcano which are younger than the great erosion time of glaciers are distributed in the direction of N70°E-S70°W. The parastic cones near the summit of the volcano are younger than those away from it. The parastic cones and the summit is arranged nearly parallel to the subduction direction of Nazca plate. The rocks from the parastic cones are calcalkaline dacitic in composition, and commonly contain augite, biotite, sanidine and plagioclase phenocrysts. Hypersthene, hornblende, quartz and sphene phenocrysts are sometimes observed. The rocks which erupted in the early stages of the parastic cone activity are more enriched in skeletal hornblende phenocrysts. The rocks in the later stage are more acidic. Plagioclase phenocrysts are classified into normal and dusty types. In dusty type, plagioclase is corroded and has dusty marginal zone and calcic, thin overgrowth rim. The dusty-type plagioclase may have been formed as the result of magma mixing. This may be supported by the presence of corroded, strongly zoned augite and of skeletal hornblende. Cognate xenolith contains plagioclase (normal-type), olivine, augite, hypersthene, biotite, sphene and cristobalite.

Aknowledgements: We would like to thank staffs of Japanese International Cooperation Agency (J.I.C.A.) and Ministries of Education, Science and Culture and Foreign Affairs in Japan who are concerned with the project of the Institute of Economic Geology at U.M.S.A. for every facilities for this study.

References

Baker, M.C.W. (1981), The nature and distribution of Upper Cenozoic ignimbrite centres in the central Andes. J. volcanol. Geotherm. Res., 11, 293-315.

DePaulo, D.J. (1981), Trace element and isotopic effects of combined wall rock assimilation and fractional crystallization. Earth planet. Sci. Let., 53, 189-202.

Eicheberger, J.C. (1978), Andesitic volcanism and crustal evolution. Nature, 275, 21-27.

Harmon, R.S., Thorpe, R.S. and Francis, P.W. (1981), Petrogenesis of Andean andesites from combined O-Sr isotope relationship. Nature, 290, 396-399.

IUGG (1971), List of the world active volcanoes with map. Special issue of Bull. Volc. Eruption. Volcanological Sciety of Japan and International Association of Volcanology and Chemistry of the Earth's Interior, 160p.

James, D.E. (1971), Andean crust and upper mantle structure. J. Geophys. Res., 76, 3246-3271.

James, D.E. (1982), A combined O, Sr, Nd and Pb isotopic and trace element study of crustal contamination in Andean lavas I. Local geochemical variations. Earth planet. Sci. Let., 57, 47-62.

Kussmaul, S., Horman, D.K., Ploskonka, E. and Subieta, T. (1977), Volcanism and structure of southwestern Bolivia. Jour. volc. Geotherm. Res., 2, 73-111.

Lefévre, C. (1973), Les caractéres magmatiques du volcanisme plio-quateraire des Andes dans la Sud du Perőu. Contr. Mineral. Petrol., 41, 259-272.

Nur, A and Ben-Avraham, Z. (1981), Volcanic gaps and the consumption of aseismic rides in south America. Geol. Soc. Am. Mem., 154, 729-740.

Phillips, W.R. and Griffen, D.T. (1981), "Optical mineralogy. The nonopaque minerals". Freemen, San Francisco, 677p.

Suwa, K., Mizutani, S, and Tsuzuki, Y. (1974), Proposed optical method of determining the twinning laws of plagioclase. Mem. Geol. Soc. Japan, 11, 167-250.

Thorpe, R.S. and Francis, P.W. (1979), Variation in Andean andesite composition and their petrogenetic significance. Tectonophys., 57, 53-70.

ボリヴィア国タケシ花崗岩体の岩石学的研究

中田節也・E.ソリア

ボリヴィア国オルロ州に分布するサハマ火山(6,542m)は，いくつかの側火山を持つcompound volcanoである。側火山はN70°E－S70°W方向に配列しており，サハマ火山の頂上に近い程活動時期が新しい。側火山の岩石はaugite － biotite daciteで，活動の古い岩石はhornblendeを多量に含む。これらの岩石はsphene斑晶を特徴的に含む。Plagioclase斑晶は普通のタイプとdusty zoneを持つタイプに分けられる。後者は異なった組成のマグマの混合によって生じたと推定される。

Estudio Petrográfico del Vocan Sajáma en Bolivia

Setsuya Nakda, E. Soria

El volcan Sajama (6,542m) está ubicado en el Departamento de Orurro, Bolivia. Este volcán es un volcano compuesto (Compound volcanos) que está formado de unos volcanos laterales. Los volcanos laterales están alineados en una dirección de N70°E-S70°W; cuanto más cerca de la cumbre de la Sajama, mas nueva es la época de la actividad del volcano. La roca de los volcanos laterales es dacita augita-biotita, y los racas mas antiguas contienen mucha cantidad de hornblenda. Estas rocas contienen caracteriticamente fenocristales de esfena. Fenocristales de plagioclasa están dividido en dos tipos, es decir, tipo normal y tipo de "dusty zone"; se puede infrir que plagioclasa del tipo de "dusty zone" fue generado de una mezcla de magmas de diferentes composiciones.

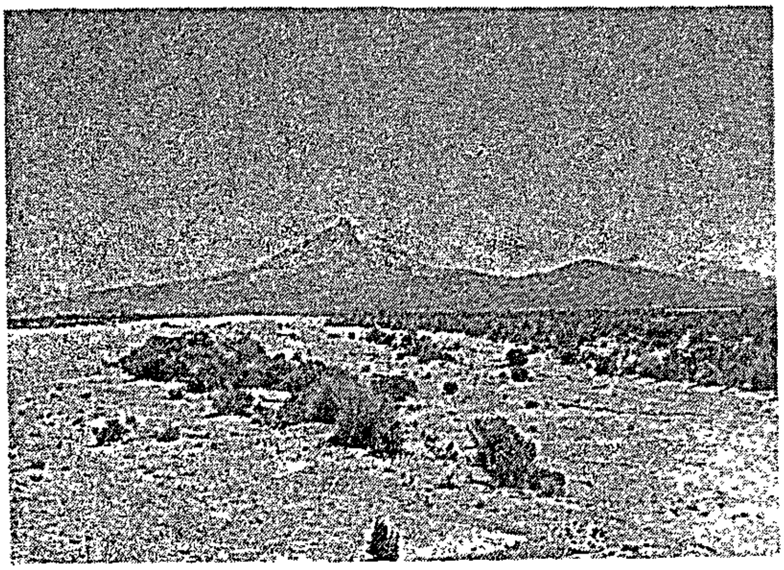

Plate-1 Eastern view of Sajama Vocano (6,542 m above sea level). Twin volcanoes covered with snow in the right hand side are Payachata Volcanoes (Parinacata (6,132 m; left) and Pomerape (6,222 m; right) which are situated on the frontier between Bolivia and Chile. The upper part of the flank of Sajama Volcano shows steep walls eroded by glaciers.

Plate-2 Northern view of Sajama Volcano. The summit is capped with glaciers and snow. In the eroded walls, interior structure of the compound stratovolcano can be seen.

Plate-3 Southern view of Sajama Volcano. Five peaks on the western slope of the volcano are Huisalla, Kohuiri Tarakkollu and Jachchasilo parastic cones, and two peaks of Chucarero parastic cone from the left to the right. Each peak of Chucarero parastic cone represents emittion point of the lavas. Huayna Potosi parastic cone rides on the middle of the eastern slope.

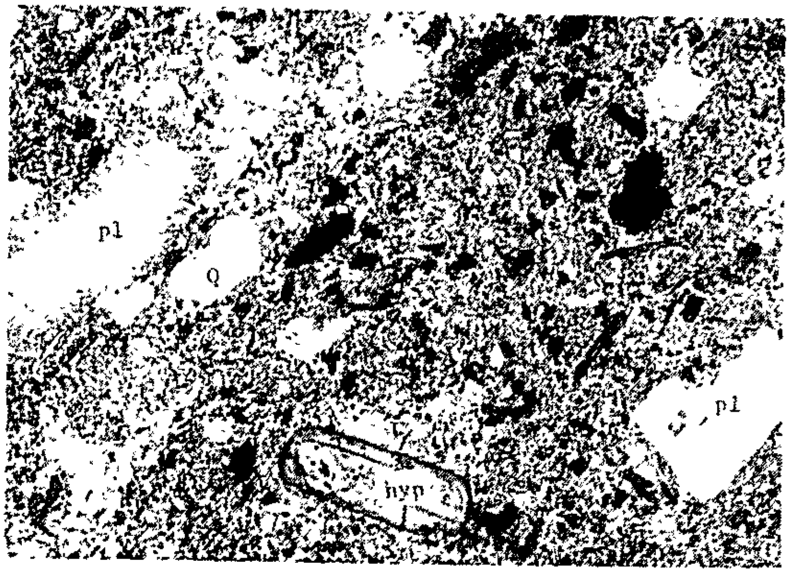

Plate-4 Microphotograph of Chucarero lava (lower nicol only). Two Kinds of plagioclase (normal and dusty types) are observed. Width of this photo is about 2 mm. Q:quartz, pl:plagioclase, hyp:hypersthene.

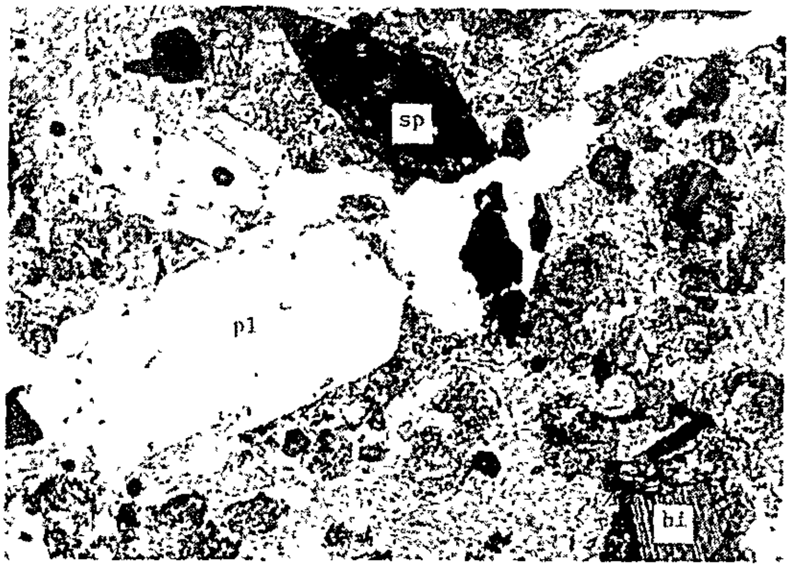

Plate-5 Microphotograph of Jachchasilo lava (lower nicol only). Sphene phenocrysts and orb texture of the glassy groundmass characterize this lava. Width of this photo is about 2 mm. sp:sphene, bi:biotite.

Plate-6 Microphotograph of Kohuiri Tarakkollu lava (lower nicol only). Sphene phenocrysts include apatite and zircon crystals. Orb texture in glassy groundmass can be seen. Width of this photo is about 2 mm. aug:augite.

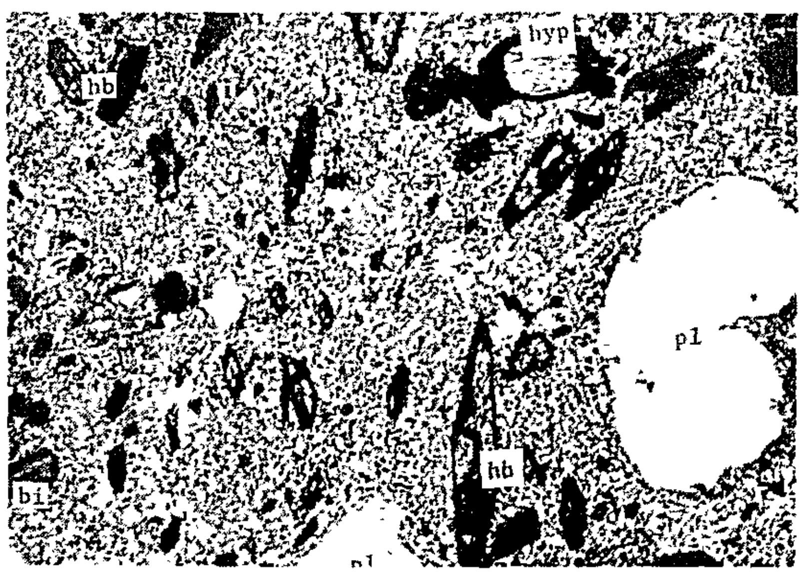

Plate-7 Microphotograph of Huisalla lava (lower nicol only). Plagioclase is dusty type. This lava is enriched in skeletal crystals of hornblende. Width of this photo is about 2 mm.

Plate-8 Microphotograph of Huincurata lave (lower nicol only). Aggregates of cristobalite are observed in intersertal groundmass. Width of this photo is about 2 mm. cr:cribtobalite.

Plate-9 Microphotograph of cognate xenolith and the host lave from Huincurata (lower nicol only). Aggregates of cristobalite are also observed in xenolith with subophitic texture. Width of this photo is about 2 mm.

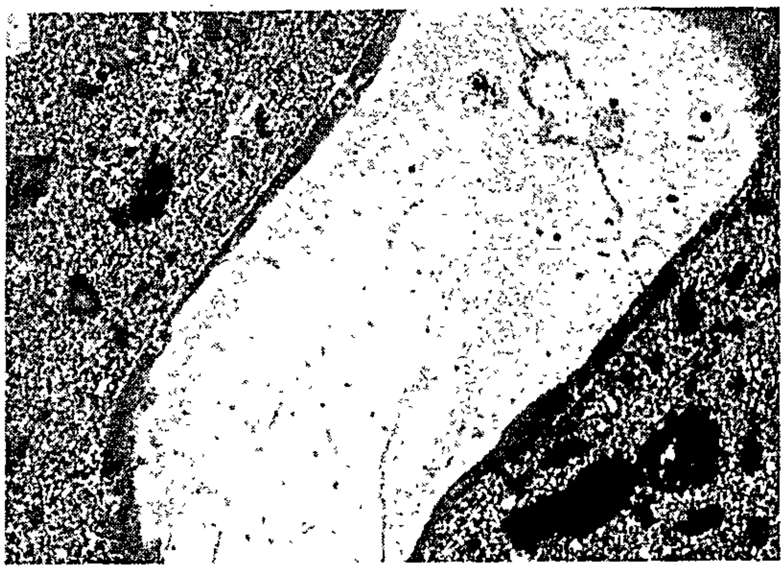

Plate-10 Microphotograph of dusty type crystal of plagioclase in Chucarero lava (lower nicol only). The crystal of plagioclase shows corrosion form. Width of this photo is about 2mm.

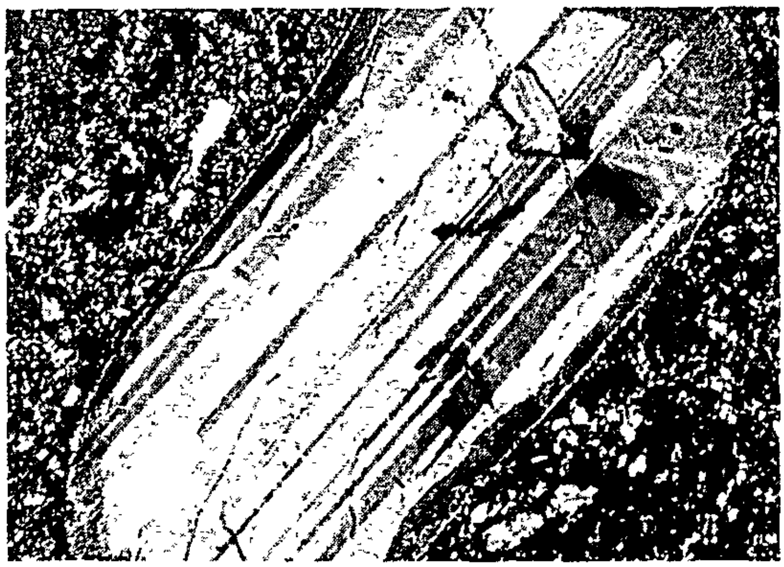

Plate-11 Microphotograph of dusty type crystal of plagioclase (crossed nicols; same in plate 10). Dusty zone in the peripheral part of the crystal is surrounded furthermore by clear, thin overgrowth rim.

Ann.Rep.JICA-IGE/UMSA
Part 2, 1, *II-45∼II-61, 1984*

Petrological Study of the Taquesi granite complex, Bolivia, and its greisenization

Alberto C. SANCHEZ

Instituto de Economica Geologica, Universidad Mayor de San Andrés, La Paz, Bolivia

Setsuya NAKADA

Department of Geology, Faculty of Science, Kyushu University, Fukuoka, 812, Japan

Abstract

Taquesi granite complex of ca.200 m.y. before present is a zoned pluton with two-mica granite/muscovite granite in the interior parts and biotite granite in the peripheral parts. Many of ore veins develop in biotite granite, and some parts of biotite granite are greisenized. Biotite granite is plagioclase porphyritic and relatively rich in Fe, Ti and Ca. Two-mica granite has similar composition to muscovite granite. It is speculated that magmas which formed the interior parts had different compositions from magmas which formed the peripheral parts. By the greisenization, elements such as F and Li were concentrated into greisenized granite, not being associated with large changes of major elements, though mineral composition of granite was largely changed.

Introduction

In the eastern Cordillera running in the direction of NE-SW in the western part of Bolivia, several granite complexes of the mesozoic and Tertiary ages were emplaced (Figure-1). The Taquesi granite complex (Mururata-Taquesi batholith of Everden et al., 1977) with the distribution area of about 130 km^2 is one of them and situated about 30 km east of La Paz. The granite complex intruded in dome-like form into the Ordovician and Silurian sedimentary rocks (Winkelmann, 1979). The K-Ar age determination of biotite from the granite complex gives 199 m.y. (Upper Triassic; Everden et al., 1977). Granitic rocks with a K-Ar age of 183 m.y. are exposed at the deep levels in the Chojlla mine located 7.5 km east of the Taquesi granite complex and in the valley of the mine area. These granitic rocks are considered to be one of the members of the Taquesi granite complex (Everden et al., 1977; Sugaki et al. 1981). Mines with W-Sn ore deposits, such as San Francisco mine, develop in the marginal part of the complex and also in the contact metamorphic area. The consitituent minerals of ore veins were described in Schneider-Scherbina (1961).

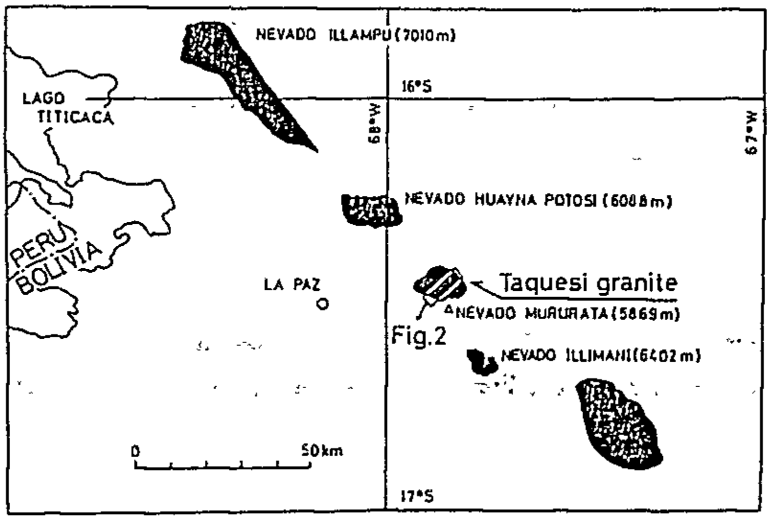

Fig. 1 Index map of the Taquesi granite complex. Solid areas represent the distribution areas of granite complexes.

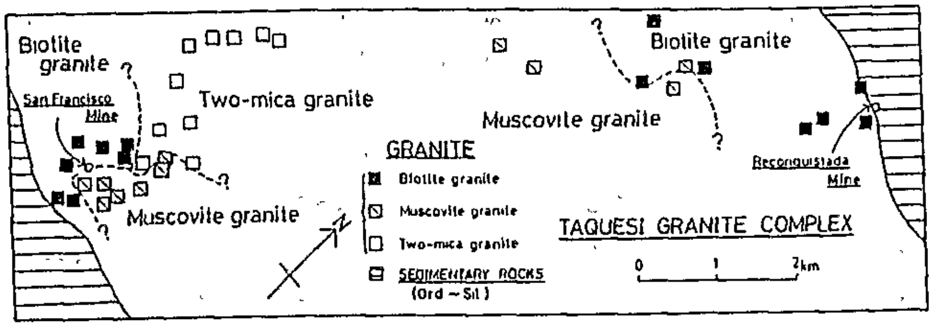

Fig. 2 Map showing granite facies of the Taquesi granit complex.

Up to now, there have been no petrological studies about this granite complex. In this paper, we will describe petrological features of the granitic rocks, and consider the nature of magma. Greisen associated with the ore veins will also be described and the greisenization in this area will be discussed. Here, greisen means the white-colored rocks composed mainly of muscovite and quartz, which make zones with the width of about 60 cm in the both sides of the ore veins.

This work was began by A.C.S. in 1979. And S.N. worked with him at Universidad Mayor de San Andrés (U.M.S.A.) in 1982 to 1983. In this paper, the unpublished data done by A.C.S. at the Freie University of Berlin in 1980 were also used for the discussion.

Petrography of the Taquesi granitic rocks

As shown in Fig. 2, rock samples were taken from the narrow area passing from San Francisco mine through the center of the complex to Reconquistada mine. Samples of greisen and sedimentary rocks were also taken from the greisen zone and the contact metamorphic area respectively. The granitic rocks were divided into three facies by the presence or the absence of biotite and muscovite; that is, biotite granite, muscovite granite and two-mica granite. The granite complex in the surveyed area contains neither pegmatitic rocks nor the eruptive equivalents to the granitic rocks.

The biotite granite occupies peripheral parts of the complex (Figure-2), and includes many ore veins and greisens. On the other hand, the muscovite and two-mica granites occupy approximately interior parts of the complex. Owing to the restricted surveyed area, the exact distribution of the three granite facies is not known. Unfortunately, the very contact or the direct intrusion relation among the three was not observed in the field. Chilled margin of the granitic rocks against the country rocks was not found. There is no relation between the width of the greisen zone (max. 100 cm) and that of the ore vein (max. 80cm, average 30cm). Films of greisen often develop, not being associated with ore veins.

Table 1 Modal analysis data of the Taquesi granitic rock and the greisen (Others: see Table 2)

	Biotite granite			Muscovite granite			Two-mica granite			Greisen
Nos.	1	13	84	2	22a	22b	34	36	42	3Va
Quartz	26.3	29.5	24.5	34.4	44.3	47.0	37.5	32.9	41.5	38.6
Plagioclase	40.0	36.5	36.4	28.8	28.5	25.1	37.0	31.8	24.1	) 1.2
K-Feldspar	18.0	23.4	21.9	22.9	16.3	14.5	15.8	25.4	22.5	
Biot/Chlorite	15.0	9.5	16.8	0.0	0.0	0.0	5.4	6.6	4.3	5.3
Muscovite	0.0	0.0	0.0	11.4	10.7	13.1	4.0	2.7	7.1	50.6
Apatite	0.8	1.1	0.2	0.8	0.3	0.3	0.0	0.5	0.2	0.9
Fluorite	0.0	0.0	0.0	0.0	0.0	0.0	0.0	0.0	0.0	1.6
Others	0.0	0.0	0.2	1.7	0.0	0.0	0.3	0.2	0.3	1.7
Total	100.1	100.0	100.0	100.0	100.0	100.0	100.0	100.1	100.0	99.9

Table 2 Description of rock-forming minerals in the Taquesi granitic rocks and the greisen

Mineral	Biotite granite	Muscovite granite	Two-mica granite	Greisen
Quartz	Anhedral;mosaic -1mm across	Anhedral;mosaic -3mm across	Anhedral;mosaic -5mm across	Anhedral;mosaic -2mm across
Plagio-clase	Euhedral-subhedral -6mm long Oscillatroy zoning (An40-An25)	Euhedral-subhedral -1.6mm long Small range of zoning (about An20)	Euhedral-subhedral -3.2mm long Small range of zoning (about An20)	Rare;anhedral -0.2mm across Including small crystals of muscovite and epidote
K-feldspar	Anhedral -2.8mm across Orthoclase(perthite) Microcline	Anhedral -2.2mm across Orthoclase(perthite)	Subhedral-anhedral -11.0mm long Orthoclase(perthite) Microcline Partly graphic texture	
Biotite	Euhedral-subhedral -1.6mm long X=pale brown Y.Z=reddish brown Partly chloritised		Euhedral-subhedral -1.4mm long Mostly chloritised Sphene,zircon and opaque minerals along the cleavage	Euhedral-subhedral -1.8mm long Mostly chloritised Opaque minerals and Muscovite along the cleavage
Muscovite		Euhedral-anhedral -3.0mm long Small euhedral crystal in plagioclase	Subhedral-anhedral -1.5mm long Small crystal in K-feldspar	Subhedral -2.0mm long Opaque minerals along the cleavage
Others	Sericite,apatite, sphene,zircon,epidote, opaque minerals	Sericite,fluorite, apatite,zircon,opaque minerals	Sericite,apatite,sphene, zircon,opaque minerals	Fluorite:-2.0mm/anhedral and among muscovite crystals. Apatite,epidote, sphene,zircon,opaque minerals

Sizes shown in this table are maximum sizes in thin sections

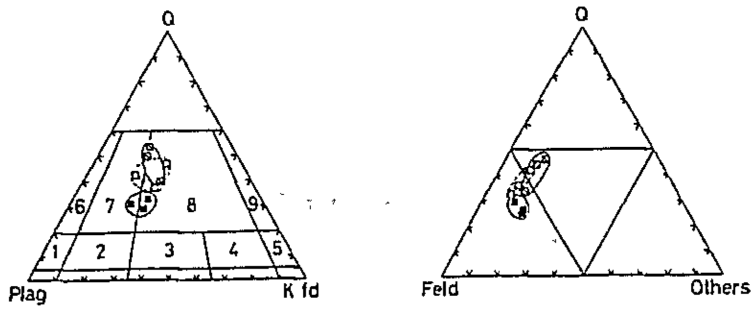

Fig. 3 Mineral compositions of the Taquesi granitic rocks. Legend is same in Fig.2. 1:quartz diorite, 2:quartz monzosyenite, 3:quartz monzonite,4:quartz syenite 5:alkali-feldspar quartz syenite, 6:tonalite, 7: granodiorite, 8:granite, 9:alkali-feldspar granite (based on the classification of I.U.G.S.1973)

Table 1 and Fig. 3 show the mineral compositions of the granitic rocks and the greisen. Table 2 lists the main characters of the rock-forming minerals. Automatic point counter of James Swift Company was used for the determination of the mineral compositions. Maximum symmetrical extinction angle method (Tsuboi, 1959; Figure-411.11) and comparing method of refractive indices of plagioclase with those of balsam and quartz (application of Figure 411.3 of Tsuboi, 1959) were used to determine the compositions of plagioclase.

The Taquesi granitic rocks are medium-grained and nearly equigranular. According to I.U.G.S. (Geotimes, Oct., 1973), the granitic rocks have the composition near the boundary between "granodiorite" and "granite". In the classification of Bateman et al. (1963), they are plotted around the boundary between "granodiorite" and "quartz monzonite (adamellite)". The biotite granite includes porphyritic crystal of plagioclase (Table 2) and has more abundance of plagioclase and less abundance of quartz than the other granite facies. The muscovite granite has the mineral composition similar to the two-mica granite, exclusive of the presence of biotite in the latter. The two-mica granite sometimes contains porphyritic crystal of orthoclase (Table 2). Composition of plagioclase in the muscovite granite is similar to that in the two-mica granite. Plagioclase only in the biotite granite shows strong oscillatory zoning, and is more calcic than those in the other granite facies. The greisen is rich in muscovite and quartz, and poor in biotite (chlorite), being compared with its host rock (biotite granite). Very small quantities of anhedral crystals of feldspar are found in the greisen.

Quartz and K-feldspar crystals are anhedral in all granite facies, exclusive of large crystal of orthoclase in the two-mica granite. Plagioclase and biotite crystals and small crystals of muscovite are euhedral to subhedral. However, large grains of muscovite are mostly anhedral, and made of aggregates of crystals grown radially. Some crystals of muscovite in the greisen develop along the cleavages of chloritized biotite, which are shown by arrangements of small grains or needles of opaque minerals. Furthermore, large crystal of muscovite in the greisen contians such arrangements of grains or needles of opaque minerals. Small, anhedral crystals of feldspar are included in mosaic quartz crystal in the greisen, and contain many minute grains of muscovite and epidote.

The abundance of opaque minerals in all granitic rocks from the Taquesi granite complex is very low (less than 0.1 vol%). Therefore, they may belong to the ilmenite-series of Ishihara's (1977) classification.

Contact metamorphic rocks taken from the area less than 1 km away from the boundary between the granitic rocks and sedimentary rocks contain white-mica, biotite, chlorite, garnet, cordierite, epidote, tourmaline, quartz and albite with small amounts of apatite and opaque minerals.

Bulk rock chemistry

Rock samples were analyzed by an atomic absorption spectrometer (Perkin Elmer Comp. Model 400), an X-ray fluorescence spectrometer (Phillips Comp. PW1212) and a fluorpotentiometer (Onion Res. Comp. MIA901). Contents of Si, Ti, Al, Fe, Ca and K were measured by the X-ray fluorescence spectrometer with the method of Flanagan (1973), and those of Ti, Al, Fe, Mn, Na, Li, Cu, Pb and Zn were by the atomic absorption spectrometer with the method of Rantala and Loring (1975). F content was determined by the fluopotentiometer with the method of Seel et al. (1964). Among major elements, content of Mg was not determined.

Table 3 shows the analytical results for granite rock facies and the greisen. All elements listed in Table 3 were not always determined for each sample. Fig. 4 shows histograms of some elements which characterize difference among the rock facies. Histograms of some elements characterizing the chemistry of greisen are also shown in Fig. 5. Fig. 6 shows some SiO_2-variation diagrams.

Table 3 Chemical analysis data of the Taquesi granitic rocks and the greisen

	Biot.gr.	Muscov.gr.	Two-mica g.	Greisen
		(in wt.%)		
SiO_2	64.4-76.4	73.3-74.8	69.5-74.9	65.0-74.3
TiO_2	0.4- 0.8	0.0- 0.3	0.1- 0.3	0.4- 0.7
Al_2O_3	9.5-16.9	12.1-15.1	12.0-15.1	12.8-15.5
Fe_2O_3#	3.2- 5.3	1.0- 5.5	1.2- 2.5	3.2- 5.9
MnO	0.03-0.07	0.02-0.06	0.01-0.07	0.06-0.08
MgO		not determined		
CaO	1.4- 2.7	0.6- 0.9	0.8- 1.3	0.9- 2.5
Na_2O	0.3- 2.2	0.1- 5.6	1.5- 2.2	0.5- 2.8
K_2O	2.5- 4.2	2.6- 5.6	4.4- 5.1	2.8- 4.7
		(in p.p.m)		
Li	50-140	15-130	50-120	240-440
F	480-1800	140-1700	300-800	3200-7100
Cu	0-110	0-88	0-130	4-120
Zn	55-290	13-410	40-600	500-1100
Pb	5-15	0-25	15-80	0-25

#:total iron as Fe_2O_3

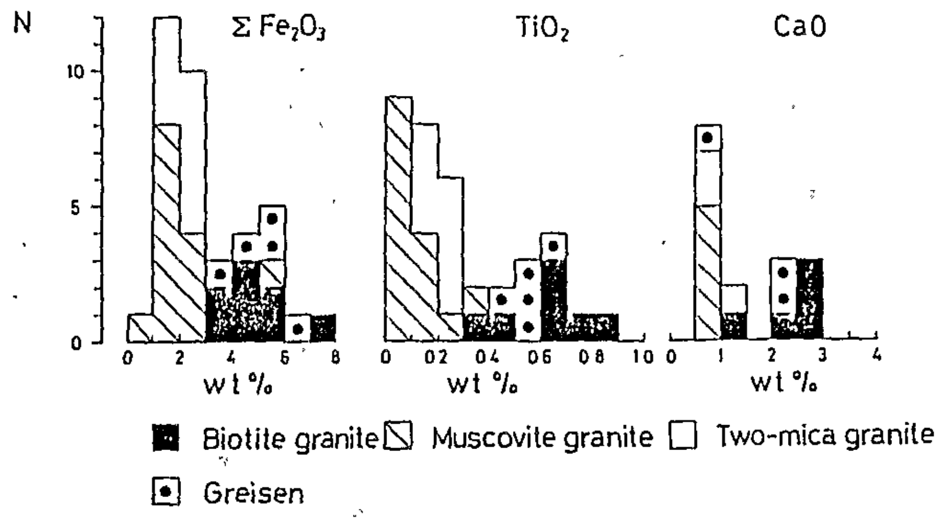

Fig. 4 Histograms of contents of Ti, Fe and Ca in the Taquesi granitic rocks and the greisen.

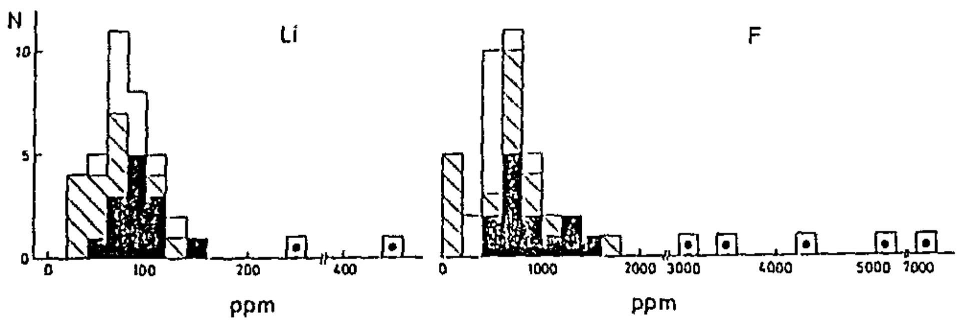

Fig. 5 Histograms of contents of Li and F in the Taquesi granitic rocks and the greisen.

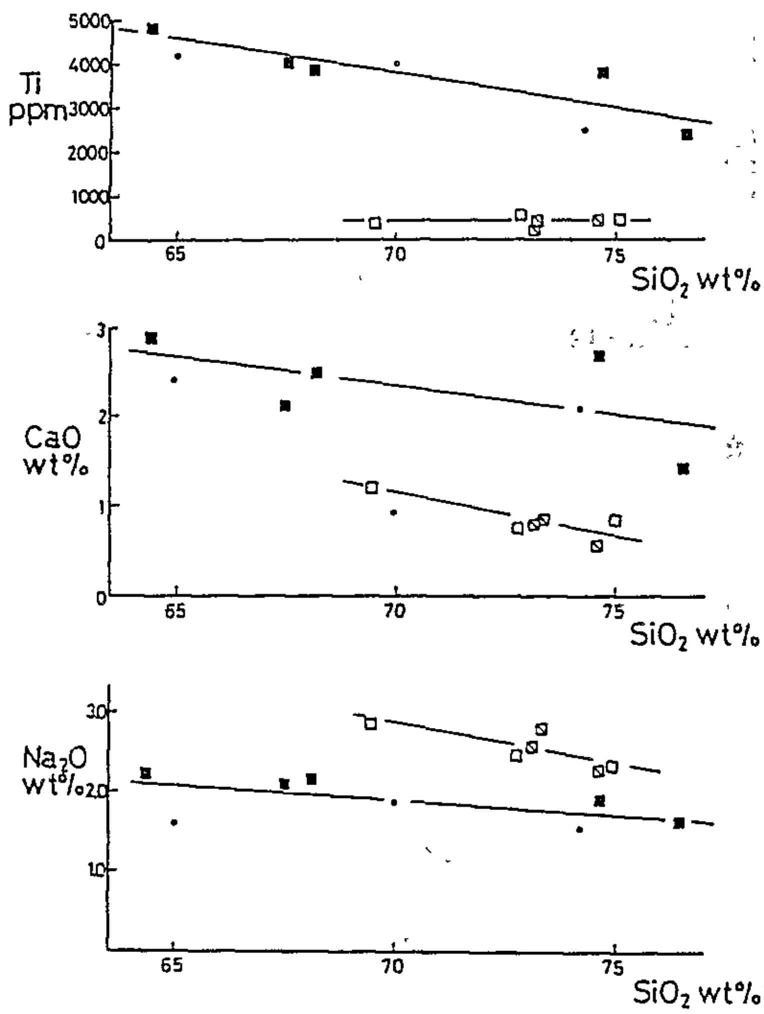

Fig. 6 SiO_2-variation diagrams of the Taquesi granitic rocks and the greisen.

The biotite granite has relatively wide range of SiO_2 content (dacite to rhyolite). The muscovite and the two-mica granites are rhyolitic in composition. The range of SiO_2 in the greisen is similar to that of the biotite granite. As shown in Fig.4, the granitic rocks are able to be divided into two groups; one group (biotite granite and greisen) is more enriched in Fe, Ti and Ca than the other group (muscovite and two-mica granites). This grouping has already been presented by the modal analysis data of the granitic rocks, though the greisen was not included in that grouping. The facts that the biotite granite has more abuncances of biotite and plagioclase than the muscovite and the two-mica granites and that the plagioclase of the former is more enriched in anorthite component than that of the latter, are reflected in the chemical difference. The two groups are also distinguished from each other in SiO_2-variation diagrams of Fig.6. The two show different variation trends in these diagrams. In respect of major elements, the greisen has the composition similar to the biotite granite. However, contents of Li and F in the greisen are very high, being compared with those in the granitic rocks (Figure 5). It seems that the greisen is, also, a little enriched in Cu and Zn (Table 3).

Discussion

The Taquesi granite complex is one of zoned plutons (e.g. Bateman and Chappell, 1979; Stephans and Halliday, 1979) in which the biotite granite occupies the peripheral parts, and the muscovite and the two-mica granites occupy the interior parts. The granitic rocks in the peripheral parts contain porphyritc crystals of plagioclase, while the interior facies lack them, and sometimes contain porphyritic crystals of orthoclase. This type of zonation is a normal style of zoned plutons (see Stephans and Halliday, 1979).

Two groups of the granitic rocks may have formed from different magmas. The observation under the microscope indicates that a magma which formed the biotite granite contained plagioclase and biotite as major phenocryst phases, while the other magma contained plagioclase, muscovite (euhedral crystals only in plagioclase grains) and biotite. The latter magma may have become to precipitate large crystal of orthoclase at the later stage of crystallization. Two kinds of variation trends in Figure 6 are able to be explained by the fractionation of biotite and relatively

Ca-rich plagioclase for the biotite granite magma and by the fractionation mainly of Na-rich plagioclase for the other magma.

Muscovite is the most popular mineral in peraluminous granitic rocks. Primary (magmatic) muscovite is one of pressure indicators of magma. According to many experimental data, muscovite is able to coexist with granitic magma at the pressure of more than 3 kb (deeper than 11 km; e.g. Clarke, 1981). If granitic magma is undersaturated with water, the lower limit of the pressure is higher (Huang and Wyllie, 1981). This indicates that, unless the euhedral muscovite crystals in the Taquesi granite were incorporated from metamorphic country rocks through the path of the magma, the Taquesi granitic magma would have generated at the considerably deep levels in the crust (more than 11 km depth). However, many of anhedral crystals in the muscovite granite or the two-mica granite may be secondary phase which was formed by the subsolidus reaction after the emplacement of the granite complex.

Judging from the mineral compositions, plagioclase, K-feldspare and small abundance of biotite in the biotite granite were replaced by quartz, muscovite and small abundance of fluorite and apatite during the greisenzation. This replacement may be suggested by muscovite crystal along the cleavages of chloritized biotite, cleavage-like lines of opaque minerals in muscovite and anhedral feldspar surviving among mosaic quartz crystals. The fact that the greisen has the major element composition similar to the host granite, indicates that major elements in the granite did not move by the greisenization. That is, the mineral replacement accompanied by the greisenization occurred in nearly closed system in respect of major elements. However, light elements such as Li and F were concentrated into the greisen zone. The time relation of the greisenization with the solidification of the host granitic magma is not clear, but the existence of aplite veins parallel to ore veins suggests that, after magma became into the solid state and became brittle, aplite intruded and, then, greisenization occurred along the cracks.

Summary

The Taquesi granite complex is a zoned pluton in which dacitic and rhyolitic magma with plagioclase and biotite occupied peripheral parts of the complex. Rhyolitic magma with Na-rich plagioclase and small abundances of muscovite and biotite intruded into the interior parts. The Taquesi granitic magma may have generated at considerably deep levels in the crust (more than 11 km depth). Greisenization occurred mainly in the peripheral parts or in the contact metamorphic area. By the greisenization, the mineral composition of the greisenized granitic rocks was completely changed, and light elements such as Li and F were concentrated into the greisenized parts. However, major elements hardly moved during the greisenization.

Acknowledgements: We would like to thank the staffs of the U.M.S.A., Japanese International Cooperation Agency (J.I.C.A.), and the Ministries of Education, Science and Culture, and Foreign Affairs in Japan, concerned with the project on the Institute of Economic Geology at U.M.S.A. for every facilities for this study. We are indebted to Prof. A. Sugaki of Tohoku University and Dr. N. Shimada of Kyushu University for giving S.N. a chance to study at U.M.S.A., and Prof. H. Schneider of Freie University of Berlin for teaching A.C.S. chemical analysis.

References

Bateman, O.C., Clark, L.D., Huber, N.K., Moore, J.G. and Rinehart, C.D. (1963), The Sierra Nevada batholith, a shythesis of recent work across the central part. U.S.geol.Surv. prof. Paper, 414-D, 146p.

Bateman, P.C. and Chappell, B.W. (1979), Crystallization, fractionation and solidification of the Tuolumne intrusive series, Yosemite National Park, California. Bull.geol.Soc. Am., 90, 465-482.

Clarke, D.B. (1981), The mineralogy of peraluminous granites, a review. Can. Mineral., 19, 3-17.

Everden, J.F., Kriz, S.J. and Cherroni, C.M. (1977), Potassium-argon ages of some Bolivia rocks. Econom. Geol., 72, 1042-1061.

Flanagan, F.J. (1973), Values for international geochemical reference samples. Geochim. Cosmochim. Acta, 37, 1989-1200.

Huang, W.L. and Wyllie, P.J. (1981), Phase relationship of S-type granite with H_2O to 35 kbar: Muscovite granite from Harney Peak, South Dakota. J. Geophy. Res., 86, 10515-10529.

Ishihara, S. (1977), The magnetite-series and imenite-series granitic rocks. Mining. Geol. Japan, 27, 293-305.

Rantala, R.T.T. and Loring, D.H. (1975), Multi-element analysis of silicate rocks and marine sediments by atomic absorption spectrometry. Atom. Absorp. Newslett., 14, 5.

Scheneider-Scherbina, A. (1961), Apuntes sobre el concepto de provincia metalifera estano Argentifera. Inst. Bolv. Petr. Tomo 2, 2, 21-29.

Seel, F., Steigner, E. and Burger, I. (1964), Ein neues verfahren zur fluor bsetimmung. Angew Chem., 532-534.

Stephans, W.E. and Halliday, A.N. (1979), Compositional variation in the Galloway plutons. In Atherton, M.P. and Tarney, J. (eds.), "Origin of granite batholiths: goechemical evidence", Shiva Pub. Lmt. Kent, 9-17.

Sugaki, A., Ueno, H., Shimada, N., Kitakaze, A., Hayashi, K., Shima, H., Sanjines, O.V. and Saavedra, A.M. (1981), Geological and mineralogical investigation on polymetallic hydrothermal deposits in Andes area of Bolivia. Rep. Overseas Sci. Res. Min. Educ., Sendai, 117 p.

Tsuboi, S. (1959), Polarized microscope. 2nd ed. (in Japanese) Iwanami Shoten, Tokyo, 305P.

Winkelmann, L. (1979), Geologic map of Cordillera Real (1:50,000) "Palca (Mururata)". Inst. Angewandte Geologie, Freie Univ., Berlin (West).

ボリヴィア国サハマ火山の岩石学的研究

A.サンチェス・中田節也

約2億年前のタケシ花崗岩体は，周縁相にbiotite graniteと内部相にtwo mica graniteとmuscovite graniteを持つzoned plutonである。biotite graniteは鉱脈に富み，greisen化をこうむっている。Biotite graniteはplagioclase porphyriticで，Fe，Ti，Caに富む。Two mica graniteとmuscovite graniteは組成的に類似している。本花崗岩体をつくったマグマの組成は，周縁相と内部相で異なっていたと推定される。Greisen化によって，花崗岩類中の鉱物組成は完全に変ったが，主要元素濃度は変化せずF，Liなどの元素が濃集した。

Estudio Petrográfico del Cuerpo Granitrico del Taquesi, La Paz, Bolivia

Alberto Sanchez, Setsuya Nakada

El cuerpo granítico del Taquesi ha sido entruido hace 200 milliones de años, es pluton zonado que tiene granito biotitico en los margenes y granito de dos micas y granito biotitica en la parte central. El granito biotitico es abundante en vetas mineralizadas y está greisenizado; este granito contiene particularmente fenocristales de plagioclasa, y es rico en Fe, Ti, y Ca. El granito de dos micas y el granito muscovítico tienen composición similar. Podemos suponer que la composción del magma que dio origen a este cuerpo granítico fue diferente en los margenes y la parte central. La composición mineralógica de los granitos ha sido completamente cambiado por greisenización, pero la concentración de los elementos no fue cambiado y presto alta concentración de F, Li, etc.

Ann.Rep. JICA/UMSA
Part II, 1, *II-62-II-70, 1984*

K-Ar ages of mineralization at the Morococala, Ávicaya, Boliver, Unificada, Chorolque and Tasna mines in Bolivia.

Hirotomo UENO and Asahiko SUGAKI

Institute of Mineralogy, Petrology and Economic Geology, Tohoku University, Sendai 980, Japan

Abstract

The K-Ar absolute ages on the clay and sulphate minerals occurring in hydrothermal veins and igneous rocks related to mineralization in Bolivia are determined. The sericite from the Morococala mine gives 20.1±1.1 Ma. The biotite age of the chualla Grande porphyry stock which has genetical relation to the mineralization in the Avicaya and Bolivar mining district is 20.5±1.0 Ma. Sulphate minerals such as alunite and jarosite give the minimum mineralization ages of 6.7, 3.9, 7.5 and 1.20 Ma for the Avicaya, Bolivar, Unificada (Potosi), Tasna and Chorolque deposits, respectively. The sericite age from the Tasna mine is 149±7 Ma, and indicates the unexpected old age.

Introduction

There are many reports on the ages of igneous rocks in Bolivia (Evernden, 1961; Clark and Farrar, 1973; Kussmaul et al., 1975; Evernden et al., 1977; Grant et al., 1979a and 1979b; JICA and MMAJ, 1977, 1978 and 1980). Some of those ages are useful to consider the ages of mineralization indirectly. The K-Ar ages on the clay and sulphate minerals which are hydrothermal alteration products and igneous rocks which have genetical relation to mineralization are described in this report.

The mineral and rock samples for the age determination were collected during our field surveys in 1977, 1979 and 1981. Figure 1 shows the location of the mines from which samples are collected. Sericite [ideal formula $KAl_2(Al\ Si_3\ O_{10})(OH)_2$], alunite [$KAl_3(SO_4)_2(OH)_6$] and jarosite [$KFe_3(SO_4)_2(OH)_6$] as potassium containing clay and sulphate minerals are separated under binoculars or by the hydraulic elutriation method. Biotite [$K(Mg, Fe)_3(Al\ Si_3\ O_{10})(OH)_2$] from igneous rocks is selected by the tapping method. Separated minerals were examined by a X-ray diffractometer. The dating procedure is done by the Teledyne Isotopes Inc. The constants for the age calculation used in this report are as follows; $^{40}K\lambda\beta=4.962\times10^{-10}/yr.$, $^{40}K\lambda e=0.581\times10^{-10}/yr.$, $^{40}K/K=0.01167$ atom% (Steiger and Jäger, 1977).

Occurrence

The occurrences of minerals are as follows.

Sericite from the Moorococala mine; Hanging wall side clay zone (sericite and kaolinite) along sphalerite-pyrite-cassiterite vein in quartzite of the Cancaniri Formation, San Francisco vein, Sub-level above 20 m from Level 190.

Biotite of the Chualla Grande stock; Granite porphyry having biotite of 0.5 to 1mm in size, Chualla Section, Level-120.

Alunite from the Avicaya mine; Alunite and kaolinite vein at the later stage of mineralization, Minchin Section, Level Loa.

Jarosite from the Bolivar mine; Within pyrite-cassiterite vein, Chica vein, Level 170.

Alunite from the Empresa Minera Unificade del Cerro de Potosi (Potosi mine); Alunite covers rock crystals within druses of quartz vein, Bolivar 2 vein, Level 0.

Sericite from the Tasna mine; Within wolframite-arsenopyrite vein, Rosario Section, Huascar vein, Level =40 Gabriel.

Jarosite and alunite from the Chorolque mine; Cementing the central part of symmetrical cassiterite vein, Fanny Ramo 1 vein, Level 6.

Result and discussion

The results of age determinations are shown in Table 1.

The sericite age of 20.1±1.1 Ma from the Morococala mine representes the exact mineralization age of Morococala ore deposits and also it is demonstrated that the mineralization has occurred in the Middle Miocene. Igneous rocks around the Morococala, Santa Fe and Japo mines give 20 to 24 Ma (Grant et al., 1979b). The sericite age is contemporaneous with those of igneous rocks.

The Chualla Grande stock which is composed of granite porphyry and called as adamellite porphyry by Sugaki et al. (1981b) gives the biotite age of 20.5±1.0 Ma. This body has genetical relation to the mineralization in the Avicaya and Bolivar mining district (Sugaki et al., 1981b). It is concluded that the mineralization in this district has occurred around 20 Ma. in Early Miocene age.

Sulphate minerals such as alunite and jarosite give 6.7±0.7, 3.9±0.7 and 12.0±0.7 Ma for the Avicaya, Bolivar and Choroloque ore deposits, respectively. These minerals may often release accumulated radiogenetic argon.. In this case they give appearently young age. Therefore, these ages represent the minimum age of each mineralization. To determine exact ages of mineralization for each ore deposit, the re-examinations by other minerals are needed.

At Tasna mine the sericite age of 149±7 Ma indicates Late Jurassic. This age differs from those of acidic igneous rocks in the Quechisla district, and also Grant et al. (1979b) reported the whole rock age of 16.4±0.3 Ma on the altered dyke at Tasna as the minimum age for the alternation of the dyke. Clearly many more datings on other minerals are needed to decide the mineralization age of the Tasna mine.

References

Evernden, J. F. (1961), Edades absolutas de algunas rocas igneas en Bolivia, por el metodo potasio-argon. Soc. Geol. Bolivia, Noticiero 2.

Evernden, J. F., Kriz, S. J. and Cherroni, M. C. (1977), Potassiumargon ages of some Bolivian rocks. Econ. Geol., 72, 1042-1061.

Grant, J. N., Halls, C., Avila, W. and Snelling, N. J. (1979a), Pottassium-argon ages of some Bolivian rocks, a discussion. Econ. Geol., 74, 702-703.

Grant, J. N., Halls, C., Avila, W. and Snelling, N. J. (1979b), Potassium-argon ageas of igneous rocks and mineralization in part of the Bolivian tin belt. Econ. Geol., 74, 838-851.

JICA (Japan International Cooperation Agency) and MMAJ (Metal Mining Agency of Japan) (1977), Informe de investigacion geologica en area San Vicente, Republica de Bolivia, 1.

JICA nad MMAJ (1978), Informe de investigacion geologica en region Sur, Republica de Bolivia, 2.

JICA nad MMAJ (1980), Informe de investigacion geologica en area Gran Chocaya, Republica de Bolivia, 1.

Kussmaul, S., Jordan, L. and Ploskonka, E. (1975), Isotope ages of Tertiary volcanic rocks of SW Bolivia. Geol. Jarb., 14, 111-120.

Steger, R. H. and Jäger, E. (1977), Subcommission on Geochronology: Convention on the use of decay constant in geo- and cosmochronology. Earth Planet. Sci. Letters, 36, 359-362.

Sugaki, A., Ueno, H., Shimada, N., Kitakaze, A., Hayashi, K., Shima, H., Sanjines, O. V. and Saavedra, A. M. (1981a), Geological study on polymetallic hydrothermal deposits in the Oruro district, Bolivia. Sci. Rept. Tohoku Univ., ser. 3, 15, 1-52.

Sugaki, A., Ueno, H. and Saavedra, A. M. (1981b), Mineralization and mineral zoning in the Avicaya and Bolivar mining district. Bolivia. Sci. Rept. Tohoku Univ. 3, 15, 53-63.

Table 1. K-Ar ages and analytical data on the Bolivian ore deposits

Sample No.	Mine	Mineral	Occurrence	K(wt%)	Rad 40Ar (cc STP/g)x10^{-5}	Rad 40Ar / Total 40Ar (%)	Age (Ma)
79100313	Morococola	Sericite	Clay Zone along sphalerite-quartz-cassiterite vein	4.61	0.359 0.366	36.1 42.1	20.1±1.1
79101121	Avicaya	Biotite	Chualla Grande Porphyry stock	6.69	0.517 0.529 0.563	43.6 49.0 46.5	20.5±1.0
AVS-31	Avicaya	Alunite	Alunite-kaolinite vein cutting cassiterite ven	5.82	0.135 0.158 0.164	23.4 26.4 27.0	6.7±0.7
BL-23	Bolivar	Jarosite	Within pyrite-cassiterite vein	7.29	0.100 0.111 0.118	14.3 14.2 20.6	3.9±0.7
8172038	Unificada (Potosi)	Alunite	Within quartz vein	6.96	0.193 0.211	19.5 15.7	7.5±1.2
8181023	Tasna	Sericite	Within wolframite-arsenopyrite vein	4.26	2.47 2.61 2.61	81.1 84.0 82.2	149±7
8180301	Chorolque	Jarosite and alunite	Within cassiterite vein	6.27	0.291 0.294	45.4 34.1	12.0±0.7

Ma is the SI unit for millions of years.

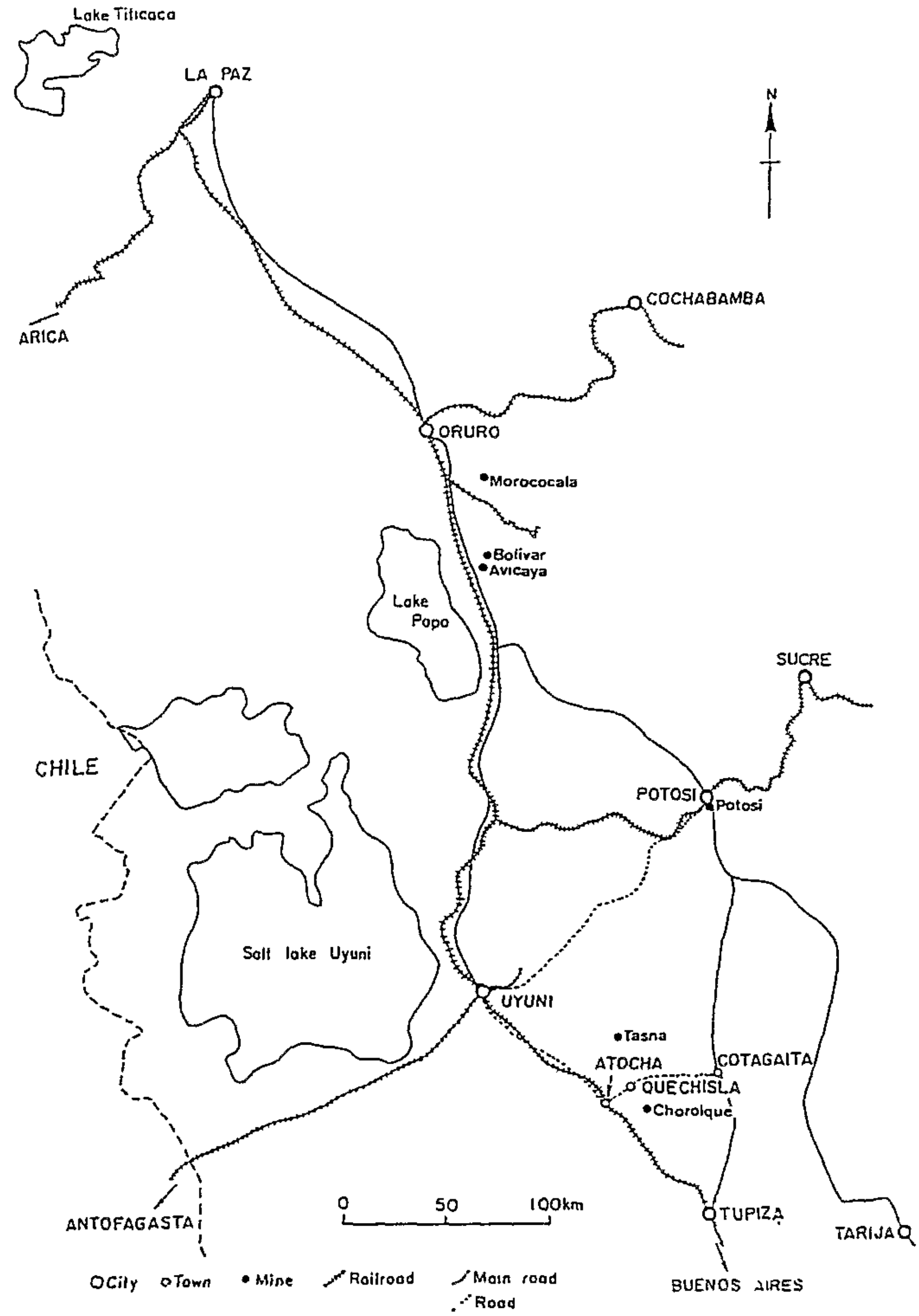

Fig. 1. Lacation of the mines investigated.

ボリヴィア国 Morococala, Avicaya, Bolivar, Unificada, Chorolque, Tasna鉱山の鉱化作用のカリウムーアルゴン年代

上野宏共，苣木浅彦

ボリヴィア国の熱水鉱脈から産する粘土鉱物などの他，鉱化作用に直接関係する火成岩についてカリウムーアルゴン法による絶対年代測定を行なった。

Morococala 鉱山産絹雲母からは２０.１±１.１Ｍａ（10^6年のＳＩ表示）の値を得た。Avicaya-Bolivar鉱床区の鉱化作用をもたらしたと考えられるChualla Grande 岩株は，２０５±１.０Ｍａである。明ばん石，ジャロサイトなどの硫酸塩鉱物からは鉱化作用の最低見積り年代が得られ，その値はAvicaya 鉱床６.７Ｍａ，Bolivar 鉱床３９Ｍａ，Unificada鉱床（別名Potosi 鉱床）７.５Ｍａ，Chorolque 鉱床１２.０Ｍａであった。Tasna鉱山からの絹雲母は１４９±７Ｍａの古い年代を得た。

この様にこれまで不確定であったこれらの鉱床の生成年代あるいはその範囲が決定された。